Manuel Nogueira
Pereira da Silva

Beamforming com Transmissão Cooperativa para Comunicações e Sensorização Integrada em Redes *Cell-Free*

Cooperative Transmit Beamforming for Integrated Sensing and Communications in Cell-Free Networks

Manuel Nogueira
Pereira da Silva

Beamforming com Transmissão Cooperativa para Comunicações e Sensorização Integrada em Redes *Cell-Free*

Cooperative Transmit Beamforming for Integrated Sensing and Communications in Cell-Free Networks

" *"In the end ?" Nothing ends, Adrian. Nothing ever ends.* "

— Dr. Manhattan, Watchmen

Universidade de Aveiro
2024

Manuel Nogueira Pereira da Silva

Beamforming com Transmissão Cooperativa para Comunicações e Sensorização Integrada em Redes *Cell-Free*

Cooperative Transmit Beamforming for Integrated Sensing and Communications in Cell-Free Networks

Dissertação apresentada à Universidade de Aveiro para cumprimento dos requisitos necessários à obtenção do grau de Mestre em Engenharia Eletrónica e Telecomunicações, realizada sob a orientação científica do Doutor Daniel Castanheira, Professor auxiliar do Departamento de Eletrónica, Telecomunicações e Informática da Universidade de Aveiro, e do Doutor Adão Silva, Professor associado do Departamento de Eletrónica, Telecomunicações e Informática da Universidade de Aveiro.

o júri / the jury

presidente / president

Prof. Doutor João Antunes da Silva
Professor associado da Faculdade de Engenharia da Universidade do Porto

vogais / examiners committee

Prof. Doutor João Antunes da Silva
Professor associado da Faculdade de Engenharia da Universidade do Porto

Prof. Doutor Daniel Filipe Marques Castanheira
Professor Auxiliar, Universidade de Aveiro (orientador)

agradecimentos / acknowledgements

O meu percurso académico culmina neste trabalho, pelo que gostaria de profundamente agradecer a várias pessoas.
Aos meus pais, irmão e família imediata pela paciência e por nunca terem deixado de acreditar nas minhas capacidades.
Ao Hugo, Bruno, André, Miguel e Eduarda por nunca me terem deixado sozinho, sendo sempre capazes de me animar, e ao João e à Teresa pela paciência e por serem os melhores ouvintes que alguém pode pedir.
Aos meus colegas (e amigos) de curso Rui, Bruno, Guilherme e Bernardo, por serem uma demonstração viva do espírito de entreajuda existente no nosso curso, e ao João Portela pelas explicações fora de aula.
Ao Professor Doutor Daniel Castanheira e ao professor Doutor Adão Silva pela disponibilidade e interesse na minha orientação ao longo do trabalho.
Para finalizar gostaria também de agradecer à Universidade de Aveiro, ao Departamento de Eletrónica, Telecomunicações e Informática e ao Instituto de Telecomunicações por garantirem as condições de trabalho e aprendizagem necessárias à realização desta dissertação.

Acknowlegment of use of AI tools /
Reconhecimento de utilização ferramentas de IA

Recognition of the use of generative Artificial Intelligence technologies and tools, software and other support tools.

I acknowledge the use of ChatGPT 3.5 and 4.0 (Open AI, https://chat.openai.com) to create initial code drafts and Grammarly (https://www.grammarly.com) for spelling and text enrichment.

Palavras Chave

Radio Detection and Raging, Integrated Sensing and Communications Orthogonal Frequency Division Multiplexing, Multiple-Input Multiple-Output, 6th Generation, Cell-Free

Resumo

A integração dos sistemas de Radio Detection and Raging (Radar) e comunicação (RadCom) tem evoluído significativamente desde a sua implementação inicial na década de 1960, quando surgiram os primeiros esquemas de radar-comunicação de dupla função (DFRC). Os investigadores da época reconheceram que a combinação de sistemas de deteção e comunicação poderia melhorar o desempenho e a eficiência energética e espectral do sistema. Esta ideia impulsionou-se na década de 1990, quando o Escritório de Pesquisa Naval dos EUA (ONR) iniciou um programa para desenvolver sistemas que estabeleceram as bases para futuros projetos baseados em sensorização integrada com comunicação (ISAC), introduzindo conceitos pioneiros na comunidade de Radar. À medida que nos aproximamos da Era do 6G, há um consenso crescente de que os sistemas de deteção desempenharão um papel crucial nos sistemas sem fios de próxima geração. A crescente proliferação de dispositivos inteligentes e as suas aplicações sublinha a importância de integrar, de forma eficiente, as funcionalidades de comunicação e Radar. Entre os vários sistemas RadCom desenvolvidos ao longo dos anos, a ISAC destaca-se por oferecer a maior eficiência espectral. A integração harmoniosa de comunicação e sensorização esta prestes a permitir uma vasta gama de aplicações inovadoras, incluindo controlo de cruzeiro colaborativo, deteção de comportamento humano, deteção de quedas e monitorização ambiental, tal como a medição de precipitação. Como tal, o objetivo desta dissertação e o desenvolvimento de uma metodologia de simulação através da técnica cooperativa de ISAC no sentido descendente (*downlink*), capaz de estimar o ângulo de um alvo. Posteriormente é realizada a avaliação do desempenho do sistema em questão. Neste trabalho são utilizados múltiplos pontos de acesso (AP) a cooperar entre si, transmitindo sinais com pré-codificadores digitais por forma a ter um sistema conjunto. Serão analisados dois cenários: no primeiro cenário o número de antenas por AP é aumentado para melhorar a resolução do Radar, no segundo cenário o número de APs é incrementado para evidenciar ganhos de diversidade.

Keywords

Radio Detection and Raging, Integrated Sensing and Communications, Orthogonal Frequency Division Multiplexing, Multiple-Input Multiple-Output, 6^{th} Generation, Cell-Free

Abstract

The integration of Radar-communications (RadCom) systems significantly evolved since its initial implementation in the 1960s, when the first Dual Functioning Radar-Communication (DFRC) schemes emerged. Early researchers recognized that combining sensing and communications could enhance performance, energy efficiency, and spectral utilization. This idea gained momentum in the 1990s, when the Office of Naval Research (ONR) initiated programs to develop integrated Radar, communications, and warfare systems, laying the groundwork for numerous Integrated Sensing and Communications (ISAC) projects. As we approach the era of 6G, there is a growing consensus that sensing will play a crucial role in next-generation wireless systems. The increasing proliferation of smart devices and applications underscores the importance of efficiently integrating communications and Radar functionalities. Among various RadCom systems developed over the years, ISAC offers the highest spectral efficiency. The seamless integration of communications and sensing is poised to enable various innovative applications, including collaborative cruise control, human behavior detection, fall detection, and environmental monitoring, such as rainfall measurement. This dissertation aims to implement a simulation chain for a cooperative technique for ISAC in the downlink direction, capable of estimating a target. Using the developed chain, the system's performance is evaluated. This work employs cooperating APs (Access Points) transmitting signals with digital precoders to achieve a joint system. To evaluate the proposed chain, two scenarios are considered: one that shows the increase of Radar resolution with the rise of AP antennas, and a second one that shows the diversity gains for a more significant number of APs.

Contents

List of Figures

List of Tables

Acronyms

1G 1st Generation. 2

2G 2nd Generation. 2

3G 3rd Generation. 3

3GPP 3rd Generation Partnership Project. 3, 4

4G 4th Generation. 3, 9

5G 5th Generation. iii, 3, 4, 9

6G 6th Generation. 1, 7, 23, 34

ADC Analog-Digital Converter. 26

AMPS Advanced Mobile Phone System. 2

AMRFC Advanced Multifunction Radio Frequency Concept. 7

AP Access Point. 1, 7, 8, 17, 18, 23–35

BER Bit Error Rate. iii, iv, 13, 29–33, 35

BS Base Station. 17, 18

CDMA Code Division Multiple Access. 2, 3

CF Cell-Free. iii, 1, 7–9, 17, 18, 23, 24, 34, 35

CP Cyclic-Prefix Block. 26

CU Central Unit. 7, 18, 23–25, 29, 33, 34

D-AMPS Digital Advanced Mobile Phone System. 2

DFRC Dual Functioning Radar-Communication. 1, 6

DL Downlink. 7

EDGE Enhanced Data-rates for GSM Evolution. 3

EGC Equal Gain Combining. 14

eMBB enhanced Mobile Broadband. 3

ESPRIT Estimation of Signal Parameters via Rotational Invariant Techniques. 35

ETSI European Telecommunications Standards Institute. 2

FDD Frequency Division Duplexing. 3

FDMA Frequency Division Multiple Access. 2

FFT Fast Fourier Transform. 11, 22, 26

GPRS General Packet Radio System. 2

GSM Global System for Communications. 2, 3

HSDPA High-Speed Downlink Packet Access. 3

HSPA High-Speed Packet Access. 3

HSUPA High-Speed Uplink Packet Access. 3

IFFT Inverse Fast Fourier Transform. 11, 12

IoT Internet of Things. 34

IS-95 CDMAOne. 2

ISAC Integrated Sensing and Communications. iii, 1, 7–9, 23–25, 34, 35

ISI Intersymbol Interference. 9, 12

ITU International Telecommunications Union. 3

LTE Long Term Evolution. 3, 4

MIMO Multiple-Input Multiple-Output. iii, 1, 3, 8, 9, 14–17, 20, 23, 24

MISO Multiple-Input Single-Output. iii, 15, 16

mm-Waves Millimiter-Waves. 4, 17, 27

mMIMO massive Multiple-Input Multiple-Output. 4, 17, 23

MMS Multimedia Message Service. 2

MMSE Minimum Mean Square Error. 7, 8, 23, 27, 34

mMTC massive Machine-Type Communication. 3

MRC Maximal Ratio Combining. 14

MTI Moving Target Indication. 6

MUSIC Multiple Signal Classification. 35

NMT Nordic Mobile Telephone. 2

NSA Non-Standalone. 4

NTT Nippon Telephone and Telegraph. 2

OFDM Orthogonal Frequency Division Multiplexing. iii, 1, 9–13, 23, 24, 26

OFDMA Orthogonal Frequency Division Multiple Access. 3

ONR Office of Naval Research. 1, 7

PDC Personal Digital Cellular. 2

PHS Personal Handy-phone System. 2

PSK Phase Shift Keying. 10

QAM Quadrature Amplitude modulation. 10, 12

Radar Radio Detection and Raging. iii, 1, 4–9, 15, 18–21, 23–25, 27, 29, 33–35

RadCom Radar-communications. 1, 6, 7

SA Standalone. 4

SAR Synthetic Aperture Radar. 6

SC Selection Combining. 14

SFBC Space-Frequency Block Coding. 14

SIMO Single-Input Multiple-Output. iii, 15, 16

SISO Single-Input Single-Output. iii, 14

SMS Short Message Service. 2

SNR Signal-to-Noise Ratio. 14–17

STBC Space-Time Block Coding. 14

TACS Total Access Communication System. 2

TDD Time Division Duplexing. 3

TDMA Time Division Multiple Access. 2

UE User Equipment. 17, 24, 26, 27

ULA Uniform Linear Array. 21

ULVA Uniform Linear Virtual Array. iii, 20

UMTS Universal Mobile Telecommunication System. 3

uRLLC ultra-Reliable and Low-Latency Communication. 3

WDCMA Wideband Code Division Multiple Access. 3

Chapter 1

Introduction

With the need to stay connected in today's fast-paced world, mobile communications have become an integral part of our daily lives, and telecommunications have made this possible. As we enter the era of Industry 5.0 and telemedicine, the importance of mobile communications to individuals and societal progress is increasing. Radio Detection and Raging (Radar) technology has proven to be crucial in various aspects of our society, such as security, weather forecasting, and transportation.

This dissertation delves into techniques that use the same wave for Radar and mobile telecommunications, ultimately leading to more efficient resource usage. This chapter explores the evolution of mobile telecommunications (as detailed chronologically in Figure 1.1 [1]) and Radar. It also outlines the goals of this dissertation and its structure.

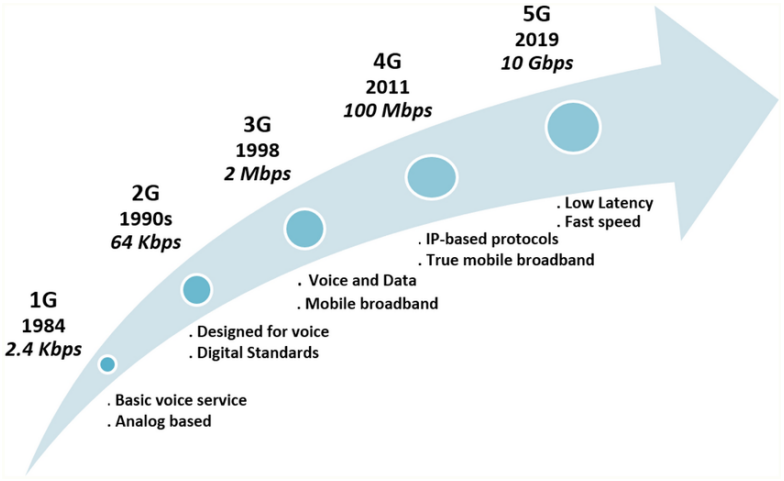

Figure 1.1: Evolution of mobile communications

1.1 Evolution of mobile communications

Before 1980, people on the move had to provide their landline phone numbers in order to be contacted. This method was deemed inconvenient, and thus, a need arose to develop a rudimentary voice service that would enable people to remain connected while on the move. In this way, a solution emerged: the 1st Generation (1G). This generation brought mobile communications, even though they were analog [2]: this means that 1G had low security [3] and wasn't robust against interference. The user's channel allocation was based on Frequency Division Multiple Access (FDMA), explained in detail in chapter 2.

The 1st Generation had different technologies [4]:

- Nippon Telephone and Telegraph (NTT, Japan);
- Nordic Mobile Telephone (NMT, mainly nordic countries);
- Total Access Communication System (TACS, Europe);
- Advanced Mobile Phone System (AMPS, USA).

Roaming was only possible if the user's carrier had service in the country they were visiting, due to the lack of standardization and proprietary carrier protocols [5].

The 2nd Generation (2G) was created in the 1990s. The main feature was digital communications, which employed the following digital channel techniques: Time Division Multiple Access (TDMA) and Code Division Multiple Access (CDMA). The switch from analog to digital communications brought greater security, less interference and higher spectral efficiency. These allowed for more users per frequency band. Over the world, different technologies were considered for the implementation of 2G [4], namely:

- Global System for Communications (GSM), the most adopted in the world, developed by the European Telecommunications Standards Institute (ETSI);
- Digital Advanced Mobile Phone System (D-AMPS), an evolution of AMPS, developed by Bell Labs and used in the USA;
- CDMAOne (IS-95), the first digital cellular technology to use CDMA, developed by Qualcomm and implemented in the USA [6];
- Personal Digital Cellular (PDC), developed by NTT DoCoMo - this standard is used in Japan alone;
- Personal Handy-phone System (PHS), developed by the NTT Laboratory in Japan.

2G also introduced data services like Short Message Service (SMS) and Multimedia Message Service (MMS), as well as improved voice quality and enhanced roaming. The 2nd Generation (2G) had two intermediate upgrades:

- 2.5G, General Packet Radio System (GPRS), uses general packet technology for more efficient and flexible internet access;

- 2.7G, Enhanced Data-rates for GSM Evolution (EDGE), introduced 8PSK, allowing for higher data-rates.

Despite never being defined as standards, 2.5G and 2.7G were considered an evolution from GSM that culminated on the 3rd Generation (3G).

The main objective of 3G was to provide higher data speeds to support more data-demanding services, such as video calls, mobile television, and Internet access [5, 4]. The 3rd Generation Partnership Project (3GPP) was formed in 1998 to address interoperability issues among networks and devices and to develop industry standards for 3G technology [7]. This resulted in several technologies being used all over the world, namely:

- Universal Mobile Telecommunication System (UMTS), used in Europe, Japan, China, and regions with predominantly GSM, which employed Wideband Code Division Multiple Access (WDCMA);
- CDMA, used in the USA.

Like the previous generation, 3G had an intermediate upgrade, named High-Speed Packet Access (HSPA). HSPA stemmed from WDCMA and had both uplink and downlink directions - High-Speed Uplink Packet Access (HSUPA) and High-Speed Downlink Packet Access (HSDPA), respectively - with increased data-rates [4].

Building on the key features of 3G, the 4th Generation (4G) has further increased data-rates to support new mobile internet and media services [4]. The most significant advancement over the previous generation was the use of full IP core networks, which enabled greater efficiency, scalability, and security [8]. The 4th Generation 3GPP standard was Long Term Evolution (LTE), employing Orthogonal Frequency Division Multiple Access (OFDMA) as the multiple access technique and Time Division Duplexing (TDD) and Frequency Division Duplexing (FDD) as the duplexing methods [9, 4]. 4G also introduced MIMO systems, which again increased spectral efficiency and coverage [9].

With the appearance 5th Generation (5G), the main goal was to support applications such as virtual and augmented reality, autonomous driving, and massive connectivity for smart cities [4]. The International Telecommunications Union (ITU) set the requirements for 5G (Figure 1.2 [10]) into three major scenarios [11, 12, 13]:

- massive Machine-Type Communication (mMTC), a massive communication link supporting several ultra-low power devices attached to the internet or communicating with each other, with or without human intervention, such as a factory sensor collecting data and transmitting it to the cloud for deep analysis;
- ultra-Reliable and Low-Latency Communication (uRLLC), designed to provide low latency (less than 1 ms) and high reliability for critical communication applications in 5G, smart grids, and intelligent transportation systems;
- enhanced Mobile Broadband (eMBB), focused on increased data-rates, being more suitable for multimedia and human-dependent services.

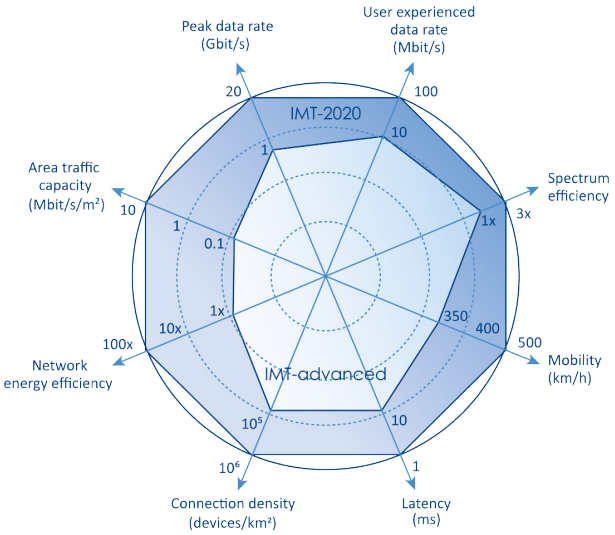

Figure 1.2: 5G Requirements

The significant technological advancements that power these three scenarios are massive Multiple-Input Multiple-Output (mMIMO) and the use of Millimiter-Waves (mmWaves) band, which consequently improved beamforming and spectral efficiency, increased data-rates, and decreased latencies [9, 4]. The standard developed by the 3GPP has two different implementations [14]:

- The Non-Standalone (NSA) standardization, completed at the end of 2017, acting as a quick evolution from the previous generation by using LTE core networks;
- The Standalone (SA) standardization, finished in June 2018, requiring its own 5G core network and providing end-to-end 5G connectivity.

NSA is easier to deploy initially because it uses the already existing LTE infrastructure, but as the 5G infrastructure increases, SA can bring better long-term benefits [14].These benefits include the delivery higher data-rates and lower latencies, as well as reduced processing overhead and power consumption due to its core network being 5G [14].

1.2 Evolution of RADAR technology

The first operating Radar device was developed in 1904 by the German inventor Christian Hülsmeyer. However, the concept was proven in 1897 by the Russian physicist Alexander Popov while watching the interference in wireless signals caused by ships [15]. This Radar sent a continuous wave with a frequency of 650 MHz, capable of detecting targets within 2 miles. This Radar was monostatic (Figure 1.3), with the transmitter sending a signal and also acting as the signal's receiver [16].

As we grew closer to World War 2, Radar saw significant developments by the British army, leading to the creation of the Chain Home Radar system in 1935 (Figure 1.4, [17]). It used long wavelengths and pulsed Radar. This system sent signals into space and measured the time it takes for the signals to return, along with other factors like the Doppler shift. This helped determine the speed, distance, and direction of the target. Due to its inherent clutter suppression characteristics, this Radar could reach a long range, making it suitable for military applications [18]. The Chain Home played a vital role in the Battle of Britain in 1940, providing early warnings of Luftwaffe raids and enabling the Royal Air Force to intercept enemy aircraft more effectively [16].

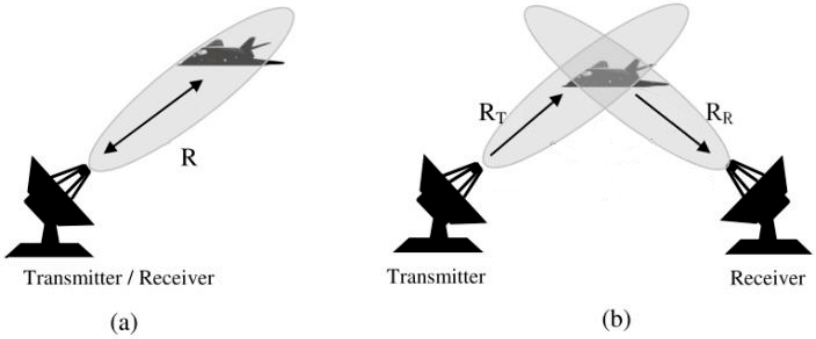

Figure 1.3: monostatic (a) and bistatic (b) radars

During that time, Appleton and Barnett conducted Ionosphere experiments and, to do so, used a bistatic configuration for the first time [19]. A bistatic configuration (Figure 1.3 [20]) uses a transmitter and a physically separated receiver [21]. Several experiments over the next few years would use bistatic principles.

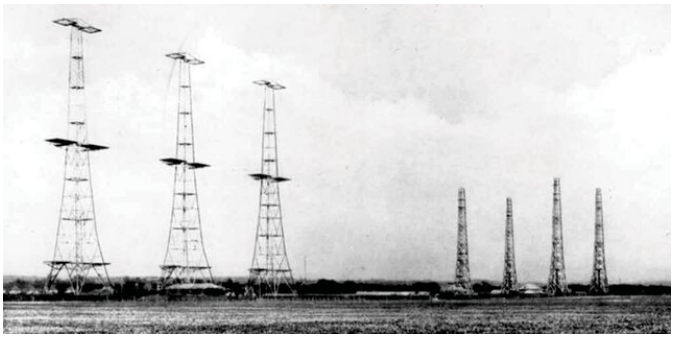

Figure 1.4: Chain Home Station

However, the first operational bistatic Radar appeared in 1943 with the Klein Heilderberg system [19]. One of the critical features of this Radar system is that it could use the ally's signals as the illumination signal. This allowed tracking and targeting without emitting its signal and thus helped to keep its secrecy [22].

After the war, the development of Radar continued and new technologies were developed.

- The Synthetic Aperture Radar (SAR) creates high-resolution images of Earth's surface by transmitting a microwave signal and recording the back-scattered signals from Earth [23].
- The Pulse-Doppler Radar, also known as Moving Target Indication (MTI) Radio Detection and Raging (Radar), uses the Doppler effect to detect radial velocity [24].
- A Monopulse Radar operates by using a monopulse antenna to generate sum and difference signals, which are then processed by a tracking receiver to estimate the orientation of a target relative to the antenna's axis [25].
- The Phased-Array Radar (Figure 1.5 [26]) employs multiple antenna elements to transmit or receive signals, arranged such that the phase of the signal from each antenna is adjusted. This allows the system to transmit or receive the signal in a specific direction without physical movement [27].

Today, Radar systems are primarily used in military, aerial and nautical guidance applications, meteorology, and remote sensing. In medicine, research is underway to use Radar (e.g. in tumour detection) [28].

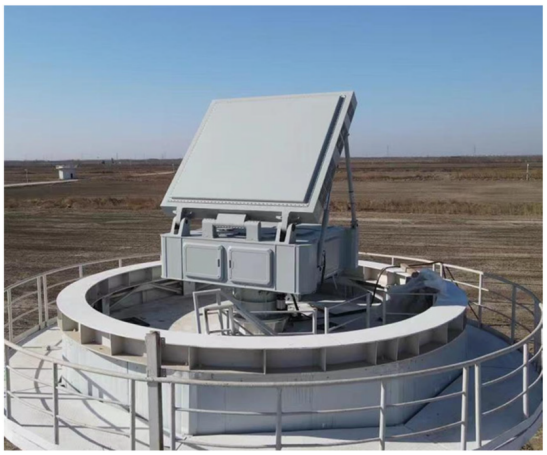

Figure 1.5: Phased-Array Radar

1.3 Motivation and objectives

The first documented implementation RadCom emerged in the 1960s as the first DFRC scheme [29]. Even before the dawn of digital communications, researchers understood that unifying sensing and communications could lead to performance gains, improved energy and spectral efficiency [30].

Research on Radar and communications gained momentum in the 1990s, and the ONR (USA) started the AMRFC program aiming to develop Radar, communications, and warfare modules [30]. This program launched several ISAC projects that would later be proposed to the Radar community, leading to pioneering ideas [30].

While the 6th Generation (6G) is still being envisioned, a common assumption is that sensing will be a more prominent feature [30]. As the number of smart devices and applications increases (Fig 1.6 [31]), the efficient integration of communications and Radar is more relevant. While this topic has been developed throughout the years with several different types of RadCom systems, ISAC offers the highest spectral efficiency compared with other systems [32]. Cell-Free (CF) networks have also been gaining more relevance as they can provide higher spectral efficiency, signal strength, and better interference management for communications [33, 34].

The integration of communications and sensing will open the door to new applications such as collaborative cruise control, human behavior detection, rainfall monitoring, and many other applications [32].

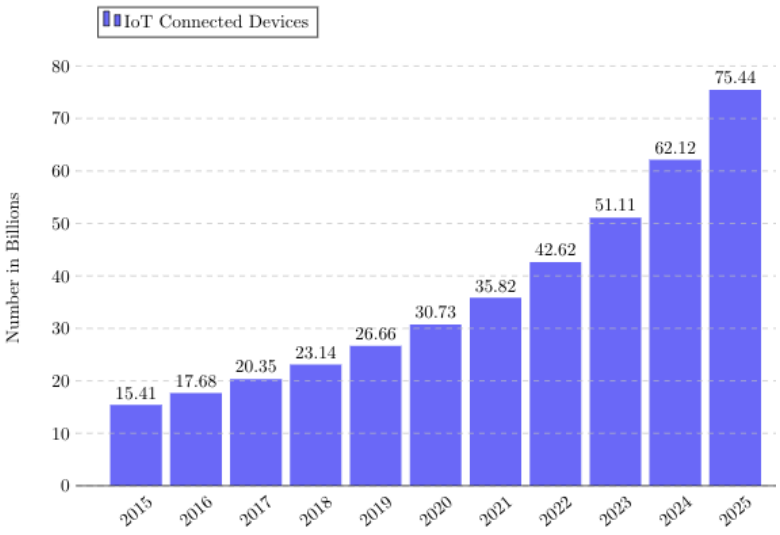

Figure 1.6: Estimated number of IoT devices until 2025

This dissertation aims to develop and evaluate the performance of a Downlink Cell-Free (CF) ISAC system, using the same communications signal for the Radar (for angle estimation). All APs in this system are connected to a Central Unit (CU). This means that the signal will be received by every AP and sent multiple times, leading to diversity gains that increase with the number of APs. The signal is divided sub-carriers that the communications part of the signal, aswell as sub-carriers that have the Radar part. For communications, digital precoding algorithm based on the Minimum Mean Square Error (MMSE) is used for signal precoding. This algorithm aims to minimize the error of the received signal. For the Radar component, the signal is multiplied by the transmitting steering vectors. The received signal is then used for the angle estimation, using the

periodogram. To evaluate the proposed system, two scenarios are evaluated: In the first scenario, the number of APs is static, while the number of antennas at each AP is increased to improve the Radar resolution. In the second scenario, the number of antennas is static, while the number of APs is increased to show diversity gains, allowing Radar signals that were previously undetected due to noise to be amplified and thus detectable.

1.4 Document structure

The remainder of this document is divided into three chapters, structured as follows:

- Chapter 2 presents the basic concepts to follow the document's contents. The first section describes the OFDM waveform for communications systems. This is followed by a section discussing MIMO systems and other different antenna configurations and their characteristics. Subsequently, the third section explains the Cell-Free concept, and the fourth section discusses the various types of diversity, while also presenting elementary Radar concepts and parameters. Finally, the last section explains the method used for the angle estimation.
- Chapter 3 presents a detailed description of the work carried out during this dissertation. Specifically, the implementation of a CF MIMO ISAC system, focusing on a design where the APs cooperate to form the ISAC transmitting signal. A digital MMSE precoder is considered at the APs for communications. At the receiver, the angles of arrival are estimated using a periodogram. Finally, simulation results are presented considering different numbers of antennas and APs to demonstrate the improved Radar detection capabilities of the cooperative ISAC system.
- Chapter 4 points out the main conclusions of this work and possible future improvements to the developed system.

Chapter 2

Theoretical Background

This chapter serves as the cornerstone for a comprehensive understanding of this dissertation. Firstly, it will delineate the fundamental principles of the used communications waveform, namely Orthogonal Frequency Division Multiplexing (OFDM). Subsequently, it will elucidate the fundamental concepts of Multiple-Input Multiple-Output (MIMO) systems. This will be succeeded by exploring the CF and diversity concepts. Finally, this chapter will elaborate on the fundamental principles of Radar systems, focusing on the angle estimation method.

2.1 OFDM

Orthogonal Frequency Division Multiplexing has been a popular digital communications scheme since its inception in 1996 [35]. It's used for 4G and 5G mobile communications, as it's robust against multipath fading by increasing spectral efficiency while being MIMO-friendly [36]. While it's not very usual to use it on Radar systems due to its limited range resolution and complexity of implementation [32], it is suitable for this work, as an ISAC system with communications capabilities is use. The next section will discuss OFDM signal characteristics.

2.1.1 Signal overview

OFDM involves using multiple sub-carriers to transmit a high-rate data stream. The process requires several sub-carriers (N) to carry the data from the source to the destination. Each sub-carrier signal is orthogonal to the others and uniformly spread in frequency, ensuring minimal Intersymbol Interference (ISI) between them. The data streams are converted into a parallel format known as an N-parallel data stream [36]. Figure 2.1 presents OFDM modulation.

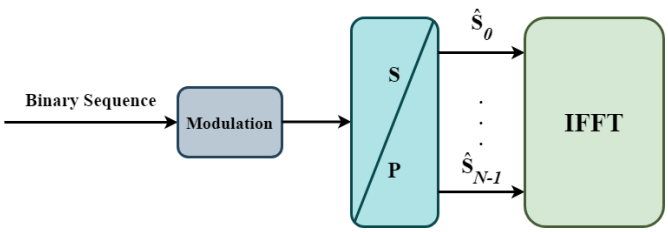

Figure 2.1: Orthogonal Frequency Division Multiplexing modulation

The generated bits are modulated using Phase Shift Keying (PSK) or Quadrature Amplitude modulation (QAM). Afterwards, each complex symbol is assigned to a sub-carrier, as seen in Figure 2.2 [37].

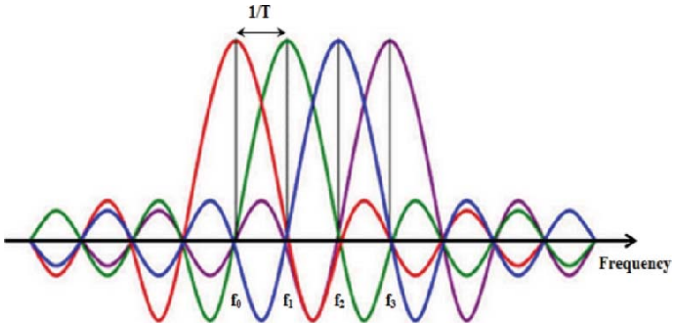

Figure 2.2: OFDM signal

Each of the complex symbols (Z) will then be transmitted in a different sub-carrier with a different frequency, from f_0 to f_{N-1}, with a specific symbol duration T [38].

The orthogonality condition can be satisfied if the sub-carriers are separated by:

$$\Delta f = \frac{1}{T} = \frac{R}{N} \tag{2.1}$$

Where T is the symbol duration, R is the symbol rate, and N is the number of sub-carriers [39].

An OFDM symbol is defined as a set of modulated sub-carriers, therefore forming an OFDM frame that is $N \times Z$, as illustrated in Figure 2.3 [40].

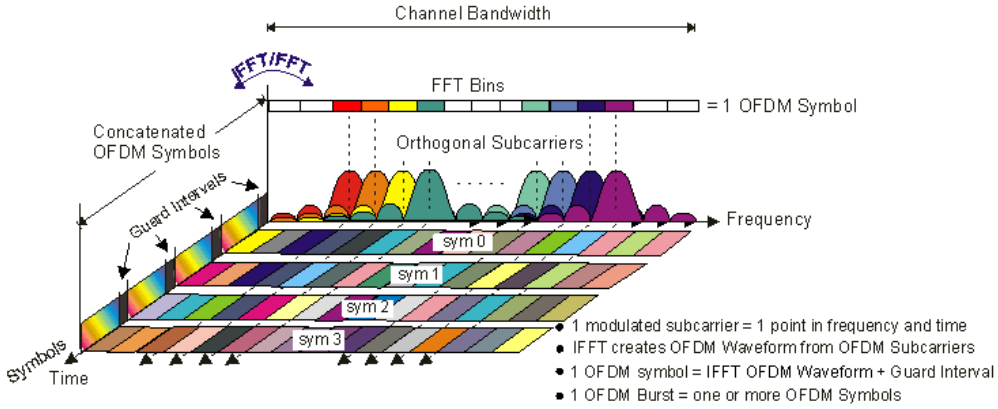

Figure 2.3: Frequency-time representation of OFDM

The Expression of the OFDM signal of the l-th OFDM symbol can be defined as:

$$s(t) = \sum_{k=0}^{N-1} d_{k,l} e^{j2\pi k \Delta f t} \tag{2.2}$$

With d_k representing the original complex symbol [39].

To increase efficiency, in this thesis, the OFDM signal was generated using Fast Fourier Transform (FFT) for modulation and Inverse Fast Fourier Transform (IFFT) for demodulation [41]. To generate the OFDM signal, an IFFT with N sub-carriers is used, with the following sampling period:

$$T_s = \frac{T}{N} \tag{2.3}$$

The sampling period replaces the time component in the discrete version:

$$s\left(\frac{nT}{N}\right) = \sum_{k=l}^{N-1} d_k e^{j2\pi k \frac{n}{N}} \tag{2.4}$$

And thus, leading us to the following [39]:

$$\{s_n\} = IFFT\{d_k\} \rightarrow \{d_k\} = FFT\{s_n\} \tag{2.5}$$

2.1.2 Orthogonality

The orthogonality in the OFDM signal makes it possible to transmit several sub-carriers simultaneously without inter-carrier interference. As long as orthogonality is maintained, retrieving the original sub-carriers is possible, even if their spectrum is overlapping [42]. If the dot product between the two signals is zero, they are orthogonal, as shown in the following condition:

$$\langle x, y \rangle = \int_0^T x(t)y(t) = 0 \tag{2.6}$$

As seen in Figure 2.2, the signal has a *sinc* response in the frequency domain. If closely observed, it can be noted that each peak for each sub-carrier matches with the null point from other sub-carriers, demonstrating the principle of orthogonality.

2.1.3 Cyclic prefix

As the channel will have multiple paths, the OFDM symbols will not be contained in the slot duration and will have an additional τ_{max} delay relative to the path. This means that there might be overlapping OFDM symbols. To safeguard the possible ISI problem, the last part of the sequence is repeated as a time guard [39]. Figure 2.4 [43] shows a representation of overlapped OFDM symbols with the cyclic prefix.

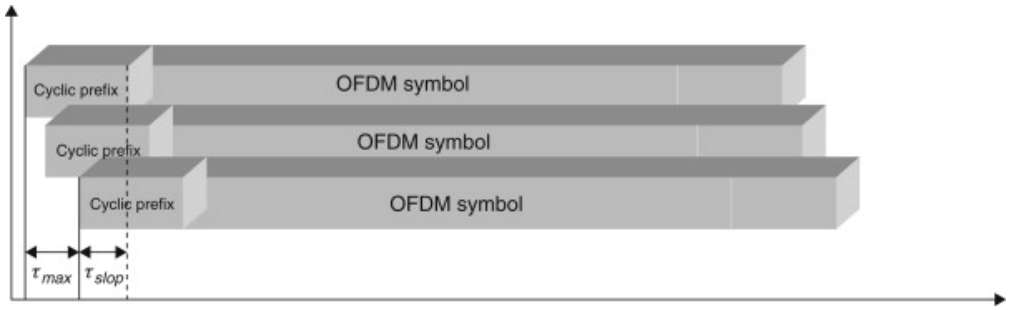

Figure 2.4: Overlapped symbols due to multiple paths in the channel

After the cyclic prefix is added to the transmitting chain, it is removed in the receiving part of the OFDM chain, as seen in the following subsection.

2.1.4 OFDM chain

On Figure 2.5, a visual representation of the OFDM chain can be seen. The first step is to modulate the binary sequence using QAM. After that, the complex symbols are converted from a serial sequence to N-parallel codes, each attributed to a sub-carrier. The next step is applying an IFFT and re-serializing the sequence, which yields our OFDM symbol - the cyclic prefix is then added.

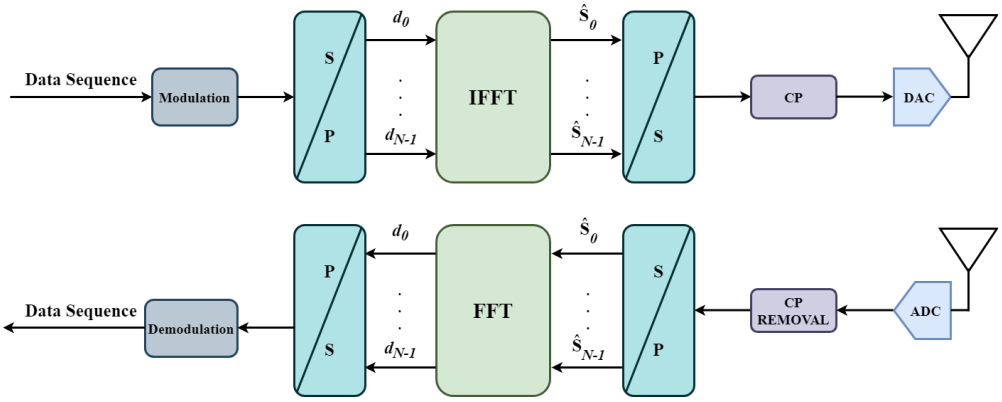

Figure 2.5: OFDM Chain

On the receiving side, the first step is to remove the cyclic prefix and then symmetrically repeat the operations applied at the transmitter - this yields the binary sequence transmitted at the start of the transmission chain.

2.2 Diversity

Fading poses a significant challenge in wireless communications. It involves multiple versions of a signal arriving at different times, resulting in interference and increasing the Bit Error Rate (BER) [44]. Several factors contribute to fading, with multipath fading being the most significant. This phenomenon is influenced by atmospheric ducting, reflection, and refraction [44].

A commonly used technique to mitigate these effects is diversity [45]. diversity involves sending the same information through uncorrelated paths. By sending repeated information through diverse paths, the environmental effects can be mitigated [39]. In the next section, three types of diversity are introduced:

- Frequency diversity is achieved by transmitting the symbol on different carrier frequencies. This method requires greater bandwidth, but it effectively maintains the transmission rate [46].
- Time diversity is achieved by sending the same symbols at different times to separate them by more than the coherence time. This type of diversity reduces the data- rate (with repetition coding) [39, 46].
- Space diversity consists of sending the information over several physical paths, using numerous transmitting and receiving antenna configurations. This configuration does not yield a higher transmission rate or bandwidth [39] [46].

The concept of space diversity involves using multiple antennas at the receiving end to combine repeated signals, which results in improved performance. This effect helps

enhance the system's ability to handle fading signals [47]. Receive diversity consists of two key concepts: diversity and antenna gain. diversity gains are based on the independence of channels and the antenna gain associated with the noise added to each receiver, which are both independent [39].

Some schemes can be used to exploit receive diversity, namely [39]:

- Maximal Ratio Combining (MRC): all paths are co-phased and summed with optimal weighting to maximize SNR;
- Equal Gain Combining (EGC): co-phases the signals but combines them with an equal weighting. It doesn't require the knowledge of channel amplitudes;
- Selection Combining (SC): selects the antenna branch with the highest Signal-to-Noise Ratio (SNR) among all received signals and is then used for detection.

In addition to receive diversity, there is also transmit diversity. Transmit diversity is similar to receive diversity, but from the perspective of transmitting [48]. To achieve this, the signal is precoded before transmission. There are two main types of transmit diversity [39]:

- Open-loop techniques do not require channel knowledge for transmission. The most common codes are Space-Time Block Coding (STBC) or Space-Frequency Block Coding (SFBC);
- Closed-loop techniques require channel knowledge for transmitting on multiple antennas [49], whether by beamforming or precoding [39].

2.3 MIMO

This section presents the characteristics of several existing antenna configurations, focusing on MIMO systems, where four configurations with different diversity gains are presented.

2.3.1 SISO, SIMO and MISO

Single-Input Single-Output (SISO) consists of one transmitting antenna and one receiving antenna (Figure 2.6). It is the simplest and cheapest configuration. However, it cannot benefit from space diversity, thus suffering from fading impact [39].

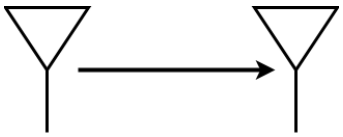

Figure 2.6: SISO configuration

For a Single-Input Multiple-Output (SIMO) system, the configuration comprises a single transmitting antenna and several receiving antennas (Figure 2.7).

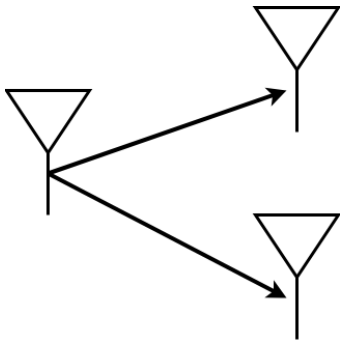

Figure 2.7: SIMO configuration

This configuration can reap the benefits of antenna and diversity gain (receive diversity), which means it can combine all of the receiving signals to maximize SNR [39]. The Multiple-Input Single-Output (MISO) configuration, inversely to SIMO, has multiple antennas on the transmitting side (Figure 2.8).

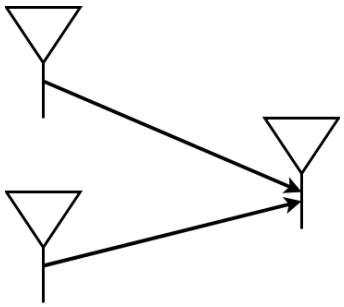

Figure 2.8: MISO configuration

This type of configuration achieves transmit diversity, as the multiple antennas are on the transmitting side [39]. This configuration is typically more complex to implement than its SIMO counterpart, as transmitting requires more complex processing and considerable power consumption.

2.3.2 MIMO

The last configuration is the one implemented in this work, MIMO, which is composed of several transmitting and receiving antennas (Figure 2.9). Despite being the most complex, it offers the highest spectral efficiency and noise resistance. MIMO enables the transmission of several data streams simultaneously through different paths using precoding, being used in this work to send different Radar and communications streams. The precoding formulations will be further elaborated in this document.

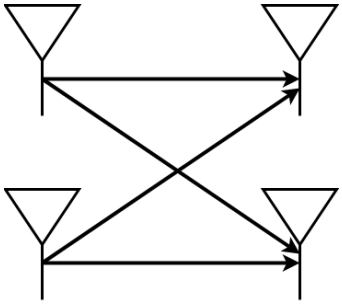

Figure 2.9: MIMO configuration

In addition to the antenna and diversity gains, which are already offered by SIMO and MISO configurations, MIMO also offers spatial multiplexing.

By leveraging the availability of the antennas on the transmitter and receiver side, Spatial multiplexing enables the transmission of multiple data streams over the same frequency channel. Each stream carries separate information, allowing for a parallel increase in data throughput [50].

There's a trade-off regarding diversity and multiplexing gains [51, 39], as shown in Figure 2.10.

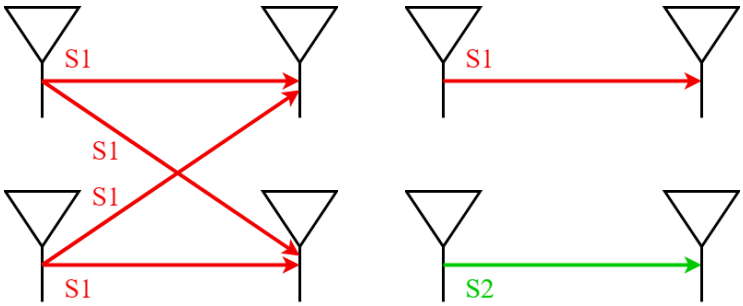

(a) Configuration with diversity gain equal to 4, and multiplexing gain 1

(b) Configuration with diversity gain equal to 1, and multiplexing gain 2

Figure 2.10: Trade-off between diversity and multiplexing gain

In case a), the diversity gain is 4, as it corresponds to $N_{tx} \times N_{rx} = 4$, and as only one symbol is transmitted, the multiplexing gain is 1. In case b), two different symbols are being sent, so we have a multiplexing gain of 2, but as two symbols are sent by two different antennas, the diversity gain takes a penalty and is reduced to 1.

The preferred setup will depend on the channel conditions. If the SNR is low, a higher diversity gain is chosen to increase signal reliability. On the other hand, if the channel conditions are good, it is better to use a higher multiplexing gain since it can improve the system transmission rates [51].

2.4 mMIMO and Cell-Free

The massive Multiple-Input Multiple-Output (mMIMO) is a type of MIMO system where a massive number of antennas is used to improve spectral efficiency, have higher reliability, and stronger resistance to interference. In this type of system, the total number of AP antennas (number of AP antennas × number of APs) is much bigger than the number of User Equipment (UE) antennas [52]. Another benefit of this technology is improved power management due to the optimized energy per bit, dynamic antenna utilization, and environment adaptation [53]. With a massive number of antennas, the beams can be much more directive, thus being narrower and able to serve distinct users while sharing the same resources, such as frequency and time, and improving spectral efficiency [54].

mMIMO uses short wavelengths - in the Millimiter-Waves (mm-Waves) band - to enable the deployment of a large number of antennas in a reduced space. This capability is fundamental to mMIMO, as it allows the implementation of a large number of antenna arrays that can serve multiple users simultaneously, enhancing capacity and performance. Another essential factor of this band is that mm-Waves frequencies (typically defined as 30 GHz to 300 GHz) offer significantly larger bandwidths than traditional sub-6 GHz bands. This increased bandwidth allows for higher data-rates and improved spectral efficiency, essential for supporting the high throughput demands of modern applications, such as video streaming, virtual reality, and others [55].

There are several types of mMIMO systems. Still, this thesis focuses on a distributed architecture, the Cell-Free (CF) model, which is different from a traditional cellular network (Figure 2.11 [56]).

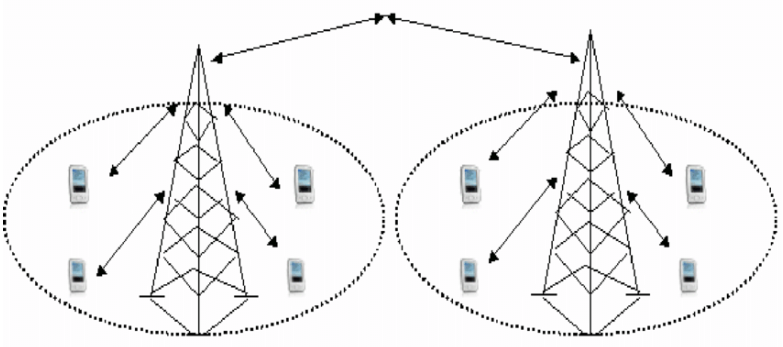

Figure 2.11: Cell based network

Signal power degrades with distance, so in a traditional cellular network, the Base Station (BS) that serves the UE is chosen according to its position within its area of coverage. A UE that is located at the cell-edge of a BS takes a 40 dB penalty in comparison with the SNR experienced at the center of the cell [34] due to inter-cell interference and hand-over problems [57]. With CF, instead of UE being served by cell towers, they're served by APs, resulting in a more uniform service [57] for all users on

the network. The fact that APs are used instead of BSs also helps network scalability [57].

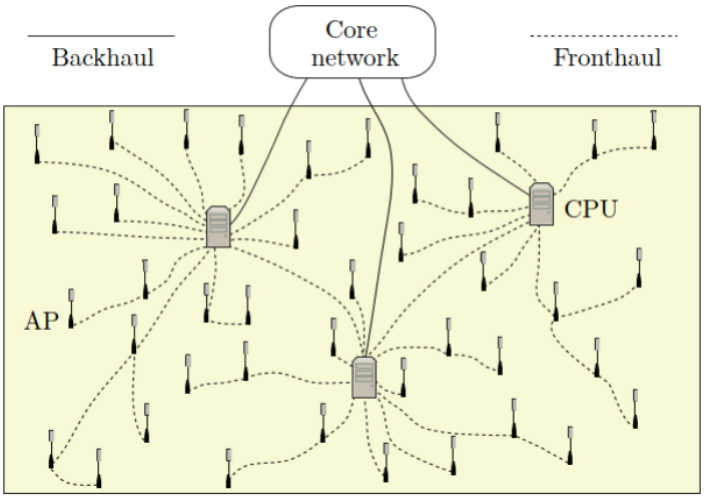

Figure 2.12: Cell-Free network

In Figure 2.12 [34], a representation of a Cell-Free (CF) network can be seen. The APs are physically connected to the CU. The CUs are then connected to the core network. The fronthaul connections provide information about the channel, while the backhaul links send or receive data to support data services [56]. In this work, the Cell-Free architecture plays a key role due to its benefits of higher spectral efficiency, higher signal strength, and better interference management [33, 34].

2.5 Radar basics

This section expounds some of the fundamentals in Radar technology, such as Radar functions, parameters, and types of Radar.

The two main categories are monostatic and bistatic Radar systems, as represented in Figure 1.3 in chapter 1. A bistatic Radar sends an electromagnetic wave to a target with one antenna and receives a reflection of the signal with another [58]. This dissertation considers a bistatic Radar, as it focuses on the angle estimation of a target.

2.5.1 Target detection

Radar signals are always subject to interference, making identifying and evaluating targets difficult. The receiver's internal noise can cause interference, as do unwanted reflections from other objects and external signals [59]. This can lead to false target detection - false alarms - or non-detection if the detection threshold isn't properly configured. Figure 2.13 [59] shows both false alarm and effective signal probabilities according

to a Gaussian distribution of the noise probability.

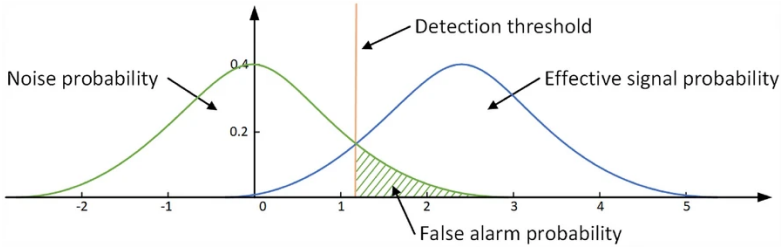

Figure 2.13: Target detection

2.5.2 Range and resolution

The range, or distance between the Radar system and the target, is determined by the time the signal takes to make the round trip to the target and back [60]. The propagation velocity of the electromagnetic wave is the speed of light ($c_0 = 3 \times 10^8$ m/s). Therefore, the range can be computed with the following Equation:

$$R = \frac{t_d \, c_0}{2} \tag{2.7}$$

Where R is the range in meters and t_d is the round-trip time in seconds.

The target resolution of a Radar is determined to distinguish two or more targets on the same bearing but at different ranges. The degree of range resolution depends on the width of the transmitted pulse and is inversely proportional to the bandwidth (B) of the transmitted signal [61].

The Equation that computes the target resolution is:

$$\Delta R = \frac{c_0}{2B} \tag{2.8}$$

2.6 Virtual array

The type of Radar used in this work is the Phased-Array Radar, chosen due to its beamforming flexibility and its integrated low-cost transceivers [62]. This model employs several antenna elements whose relative phase varies, allowing to steer the beam in the desired direction [63]. Figure 2.14 [63] shows a representation of this system.

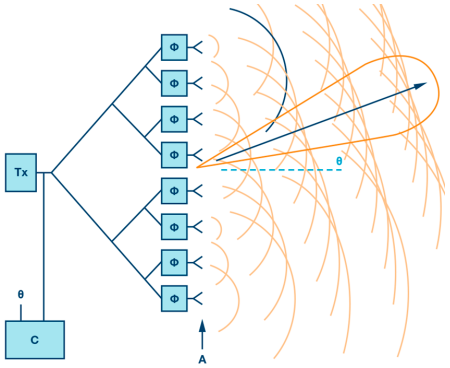

Figure 2.14: Phased-Array

The virtual array technique is used in antenna systems to increase the effective number of antennas without physically adding more. This is achieved by exploiting signal processing, which involves mathematically combining the transmitting antennas with the receiving antennas, in a way that resembles a convolution. The received signals are treated as from a more extensive antenna array. This method is beneficial in MIMO systems, where it helps improve spatial resolution and capacity without additional hardware [64].

Suppose a spatial path is defined from a specific P-th antenna to the target and back to a R-th antenna, considering that this system is MIMO and uses P transmitting antennas and Q receiving antennas. Using this technique, spatial diversity gains can be used to increase the number of spatial paths to $P \times Q$ [64]. In a typical array Radar, the antennas are inter-element spaced by $\lambda/2$. However, this results in several repeated responses due to having the same phase. To achieve the maximum number of different paths, the distance between the transmitting antennas must be $Q \times \lambda/2$, for a distance of $\lambda/2$ between the receiving antennas. The result can be seen in Figure 2.15, using a Uniform Linear Virtual Array (ULVA).

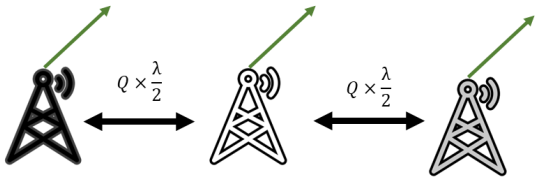

(a) Physical Transmit Array

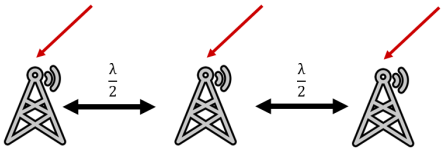

(b) Physical Receive Array

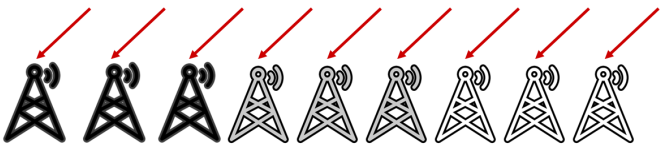

(c) Virtual Array

Figure 2.15: ULVA MIMO Radar system with its virtual array

2.7 Angle estimation

Angle estimation requires at least two receiving antennas (bistatic configuration). Figure 2.16 shows a scenario with one transmitting antenna and two receiving antennas.

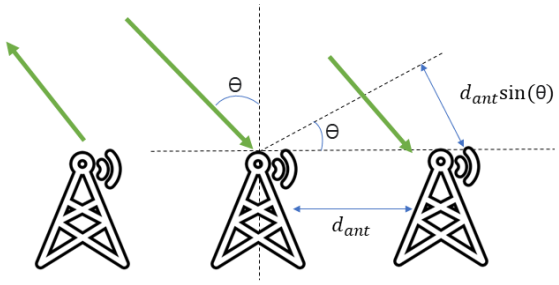

Figure 2.16: Angle estimation

The signal from the transmitting antenna is reflected by the target and received by the receiving antennas. This signal travels an additional distance of $d_{ant}\sin(\theta)$, which causes a phase difference between the two received signals, corresponding to:

$$w = \frac{2\pi}{\lambda} d \sin(\theta) \tag{2.9}$$

The phase increases linearly with the antenna index for an ULA, allowing the estimation of the angle using the periodogram. Due to this phase difference, the range will fall between -90º and 90º [65]. The angle resolution corresponds to the minimum target separation to perform a correct estimation [66] and can be expressed as:

$$\Delta\theta = \frac{\lambda}{PQ\, d_{ant} \cos(\theta)} \tag{2.10}$$

Where λ is the wavelength of the signal, P is the number of transmitting antennas, Q is the number of receiving antennas, and d_{ant} is the distance between the antennas.

2.8 Periodogram

For the one-dimensional case of identifying sinusoids in a discrete-time signal, the periodogram is a well understood tool for developing Radar imaging [67]. For a given discrete signal $s(k)$ with N samples the periodogram is obtained as follows:

$$Per_{s(k)}(f) = \frac{1}{N} \left| \sum_{k=0}^{N-1} s(k) e^{-j2\pi f k} \right|^2 \tag{2.11}$$

However, in digital systems, the most common way to compute this is to quantize the frequency in regular intervals and use the FFT [67].

$$Per_{s(k)}(f) = \frac{1}{N}\left|\sum_{k=0}^{N-1} s(k)e^{-j2\pi\frac{nk}{N_{per}}}\right|^2 \tag{2.12}$$

$$= \frac{1}{N}\left|FFT_{N_{Per}}[s(k)]\right|^2 \tag{2.13}$$

Where $FFT_{N_{Per}}[s(k)]$ is the FFT of length N_{per} of the signal $s(k)$. N_{per} corresponds to the number of supporting points for the periodogram and is typically equal to or greater than the number of samples (N).

The periodogram Expression above will be further expanded in the next chapter.

Chapter 3

Implemented ISAC system with cooperative beamforming

As research on 6G continues, one of the most prominent technologies is ISAC. At the same time, development on CF-mMIMO is ongoing as a promising solution to mitigate inter-cell interference.

An ISAC system is a wireless network architecture that simultaneously performs sensing and communications tasks using shared resources. It integrates the functionalities of detecting environmental data and transmitting information, enhancing overall efficiency. ISAC leverages the interaction between sensing and communications for mutual benefits, optimizing performance for both functions. It is adaptable to various applications, including smart cities and vehicular networks. Advanced signal processing techniques are employed to effectively manage trade-offs between sensing and communications [30].

This chapter presents in detail the implementation and simulation results of a downlink Cell-Free OFDM MIMO ISAC system. The primary goal is to leverage the cooperative capabilities of APs to enhance both communications and Radar functionalities within the network. The signal is divided into two sets of sub-carriers: the first set carries the communications precoded signal and the second carries the Radar precoded signal.

For the communications part, a digital MMSE precoder is employed, designed to optimize the transmitted signal by using the cooperation among APs. Regarding the architecture of a CF system, it is assumed that each AP has access to real-time channel state information, as they are all connected to the same CU. For the Radar component, the precoder is constructed using a transmitting steering vector, which plays a pivotal role in directing the transmitted signals toward the target of interest. When this steering vector is applied to the Radar channel, it is easier to compute the angle of arrival of the reflected signals from the target. The periodogram then uses the reflected signals to estimate the target's angle by analyzing power peaks in the [-90^o, 90^o] range.

The simulation results are presented for two scenarios: in the first one, a single AP is used, and the number of antennas is increased to improve angle resolution; in the second scenario, 64 antennas are used with an increase in the number of APs, showcasing

improved Radar detection capabilities of the cooperative ISAC system, allowing Radar signals that were previously undetected due to noise to be amplified and thus detectable.

The present chapter starts by discussing the system model and architecture considered for the implementation. Subsequently, the simulation results for the two scenarios, each with three cases, are presented. Finally, the results are analyzed to evaluate the system's performance.

3.1 Architecture

The architecture considered in this dissertation is based on a CF MIMO system, which is composed of M APs and U User Equipment (UE)s. Randomly and uniformly distributed over a determined region, the APs incorporate N_{tx} transmitting and N_{rx} receiving antennas, while the UEs incorporate N_{ue} antennas. Through a fronthaul connection, the CU forwards the data signals to the APs, which then precode the received data to generate the transmitted signal. In Figure 3.1, an example of a CF network with M APs (connected to CU) and U UEs can be seen. The signals transmitted from the APs are used to estimate the target's position. The target reflects these signals, with a specific gain, to a receiving AP, where the angle of the target is estimated.

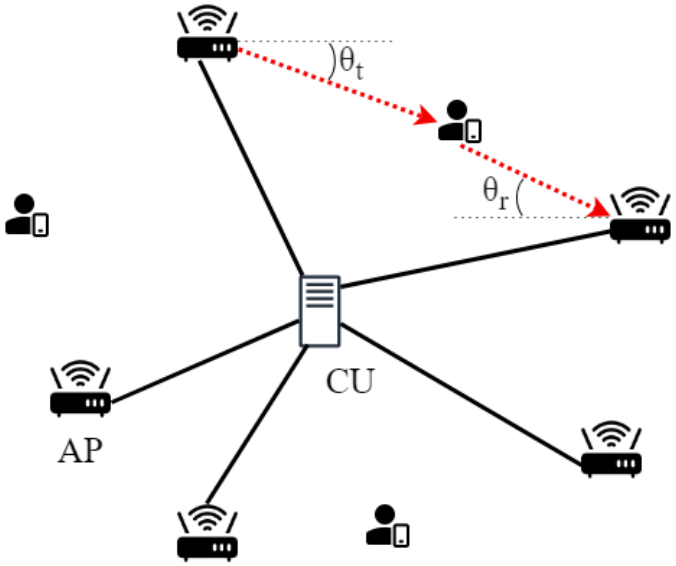

Figure 3.1: ISAC Cell-Free Network

The employed modulation scheme is OFDM with sub-carrier division, since some are used for communications and others for Radar, as seen in Figure 3.2.

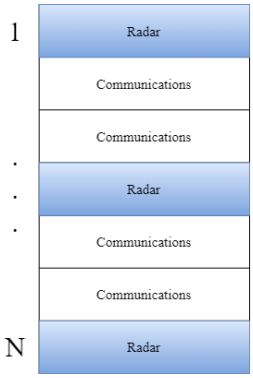

Figure 3.2: Sub-carrier division

In the following subsections, the communications system model is presented first, followed by the details of the Radar system model.

3.2 Communications system model

For the development of this work, the ISAC system model has been implemented in the architecture.

3.2.1 Transmitted signal

From Figure 3.3, the transmitting diagram can be observed, composed by the CU and the APs. Each AP contains N_{tx} transmitting antennas, and the signal transmitted by the m-th AP at the k-th carrier is given by:

$$\mathbf{x}_{m,k} = \mathbf{W}_{m,k}\mathbf{s}_k \tag{3.1}$$

Where $\mathbf{x}_{m,k} \in \mathbb{C}^{N_{tx}\times 1}$ is the transmitted signal from the m-th AP at the k-th carrier, $\mathbf{W}_{m,k} \in \mathbb{C}^{N_{tx}\times U}$ is the digital precoder at the m-th AP and k-th carrier, and $\mathbf{s}_k \in \mathbb{C}^{U\times 1}$ is the data at the k-th carrier. Every AP is connected to the CU through a fronthaul connection. The data sent from one AP is known by every AP, as they are all connected to the same CU. As a result, the data is sent repeatedly by different AP, thus increasing the signal reliability. Figure 3.3 shows the block diagram for the CU and AP blocks. Each AP will have access to U different bit streams. Before being transmitted, these bit streams will then be multiplied by the precoder $\mathbf{W}_{m,k}$.

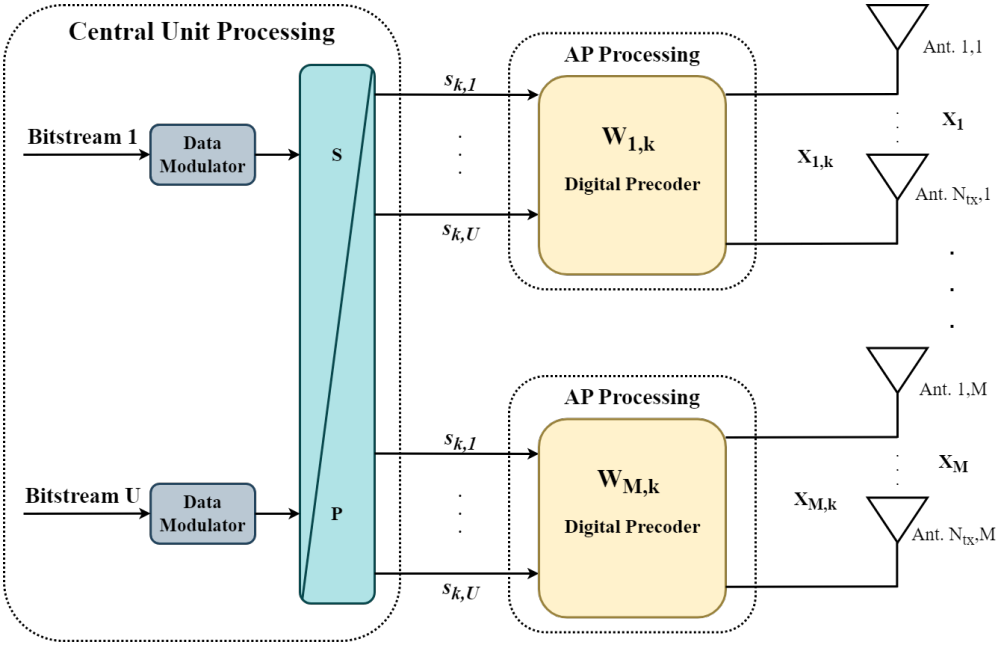

Figure 3.3: Distributed transmitter block diagram (downlink)

At the UE, the received signal $\mathbf{s}_k$ is processed through the OFDM chain, as depicted in Figure 3.4.

First, the ADC converts the received signal from the analog to the digital domain. Then, the CP is removed and the serial-parallel block takes the serial data stream. Then, the data stream is splitted into several parallel streams, enabling parallel processing and allowing each sub-carrier to handle a portion of the data stream. The next stage is the FFT block, which converts the signal from the time domain to the frequency domain for processing purposes. The parallel-serial block then consolidates the parallel data streams into a single serial stream, and the resulting signal passes through the combiner, which cancels the effects of the channel by combining the data from each AP to optimize performance. Finally, the demodulation block converts the equalized signal into a binary sequence.

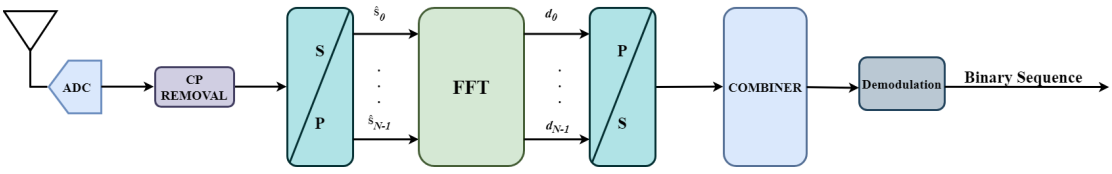

Figure 3.4: User terminal block diagram (downlink)

The signal received at the UE is the sum of all signals from every AP is given by:

$$\mathbf{Y}_{u,k} = \sum_{\mathbf{m=1}}^{\mathbf{M}} \mathbf{h}_{m,u,k}\, \mathbf{x}_{m,k} + \mathbf{n}_k \tag{3.2}$$

The channel between the m-th AP and u-th UE is denoted by $\mathbf{h}_{m,u,k} \in \mathbb{C}^{1\times N_{\text{tx}}}$, where N_{tx} is the number of transmitting antennas. The transmitted signal is represented by $\mathbf{x}_{m,k} \in \mathbb{C}^{N_{tx}\times 1}$, and the additive Gaussian noise by $\mathbf{n}_k \in \mathbb{C}^{N_{tx}}$

Precoder design

This work considers a fully digital precoder; although a hybrid precoder is often used in the mm-Waves to reduce power consumption, its implementation is far more complex.

The digital precoder $\mathbf{W}_{m,k} \in \mathbb{C}^{N_{tx}\times U}$ is computed using the MMSE method [39]:

$$\mathbf{W}_{m,k} = \mathbf{H}_{m,k}^{H} \left(\mathbf{H}_{m,k}\, \mathbf{H}_{m,k}^{H} + \sigma^2\, \mathbf{I}_U\right)^{-1} \tag{3.3}$$

Where the matrix $\mathbf{H}_{m,k}$ is comprised of U elements of the $\mathbf{h}_{m,u,k}$.

To normalize the power for each stream:

$$\mathbf{P} = \text{DIAG}(\mathbf{W}_{m,k}^{H}\, \mathbf{W}_{m,k}) \tag{3.4}$$

Finally, the precoder is given by:

$$\hat{\mathbf{W}}_{m,k} = \frac{\mathbf{W}_{m,k}}{\sqrt{\text{DIAG}(\mathbf{P})}} \tag{3.5}$$

3.3 Radar system model

This section introduces the Radar system model.

3.3.1 Transmitted and received signal

At the m-th transmitter, the AP forms the signal along the direction θ_t of the target. The transmitted signal $\mathbf{x}_m$ is given by:

$$\mathbf{x}_m = \mathbf{W}_R\, \mathbf{s}_k \tag{3.6}$$

Where $\mathbf{W}_R$ is the Radar precoder and $\mathbf{s}_k$ is a data symbol transmitted by the APs.

The received signal $\mathbf{y}_R$ (after being reflected by the target) at the receiving AP will be the sum of received signals sent by all transmitting APs, and is expressed by:

$$\mathbf{y}_R = \sum_{\mathbf{m=1}}^{\mathbf{M}} \mathbf{F}_m\, \mathbf{x}_m \tag{3.7}$$

Where $\mathbf{F}_m$ represents the Radar channel. The details of this channel, along with the precoder for the Radar component, will be discussed in the following subsection.

3.3.2 Channel description

To represent the channel propagation from the transmitting antennas to any target and vice-versa, the following Expressions were used to compute the steering vectors for transmission and reception, $\mathbf{a}_T(\theta_t) \in \mathbb{C}^{N_{\text{tx}} \times 1}$ and $\mathbf{a}_R(\theta_r) \in \mathbb{C}^{N_{\text{rx}} \times 1}$ [68], assuming the target is in line of sight with the APs :

$$\mathbf{a}_T(\theta_t) = \frac{1}{\sqrt{N_{\text{tx}}}} \begin{bmatrix} 1 \\ e^{-j\frac{2\pi}{\lambda} d \sin(\theta_t)} \\ e^{-j2\frac{2\pi}{\lambda} d \sin(\theta_t)} \\ \vdots \\ e^{-j(N_{\text{tx}}-1)\frac{2\pi}{\lambda} d \sin(\theta_t)} \end{bmatrix} \tag{3.8}$$

$$\mathbf{a}_R(\theta_r) = \frac{1}{\sqrt{N_{\text{rx}}}} \begin{bmatrix} 1 \\ e^{-j\frac{2\pi}{\lambda} d \sin(\theta_r)} \\ e^{-j2\frac{2\pi}{\lambda} d \sin(\theta_r)} \\ \vdots \\ e^{-j(N_{\text{rx}}-1)\frac{2\pi}{\lambda} d \sin(\theta_r)} \end{bmatrix} \tag{3.9}$$

The transmission and reception channel $\mathbf{F}_m \in \mathbb{C}^{N_{\text{tx}} \times N_{\text{rx}}}$ (Figure 3.5) for the AP can be precisely determined using the following Expression:

$$\mathbf{F}_m = \mathbf{a}_R(\theta_r)\, r\, \mathbf{a}_T(\theta_t)^H \tag{3.10}$$

Where θ_r denotes the angle between the target and the receiving AP, θ_t the angle between the target and the m-th transmitting AP, and r represents a reflectivity gain, which means that each target can reflect more or less depending on the conditions surrounding the target and its material.

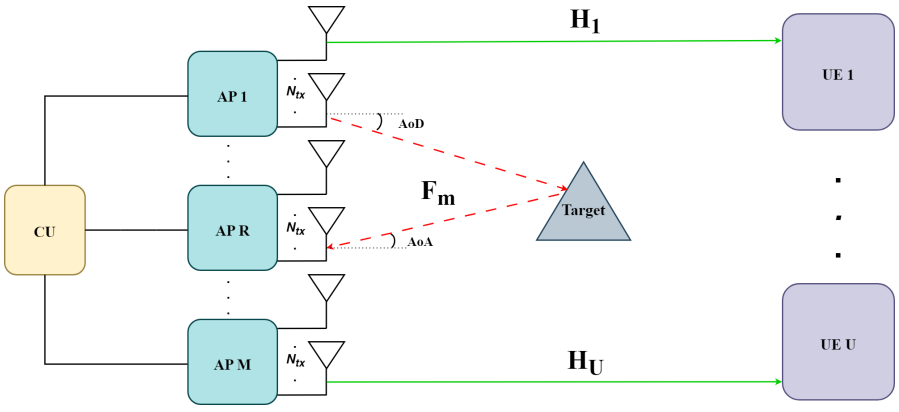

Figure 3.5: Radar architecture overview

As a consequence of the Radar channel being formulated as it is, the precoder $\mathbf{W}_R$ steers a signal in the direction of the target, thus taking the following form:

$$\mathbf{W}_R = \mathbf{a}_T(\theta_t) \tag{3.11}$$

When the precoder is multiplied by the channel, it mathematically eliminates the transmitting steering vector component $\mathbf{a}_T$, leaving the receiving steering vector $\mathbf{a}_R$ along with the sent data. Elaborating the Expression (3.7) :

$$\mathbf{y}_R = \sum_{\mathbf{m=1}}^{\mathbf{M}} \mathbf{F}_m \, \mathbf{x}_m = \sum_{\mathbf{m=1}}^{\mathbf{M}} r \, \mathbf{a}_R \, \mathbf{a}_T{}^H \mathbf{a}_T \, \mathbf{s}_k = \sum_{\mathbf{m=1}}^{\mathbf{M}} r \, \mathbf{a}_R \, \mathbf{s}_k \tag{3.12}$$

As every AP is connected to the same CU, the information is shared. This leaves only the steering vector $\mathbf{a}_R$, making it possible to compute the angle of arrival (Figure 3.5).

3.3.3 Receiving access point processing

As mentioned before, the periodogram can be used to obtain Radar imaging. In most cases, it is used in the frequency domain to estimate the most likely sinusoids.

However, this work aims to estimate the target angle, so the periodogram will vary according to the angle. As the steering vector $\mathbf{a}_R$ and received signal $\mathbf{y}_R$ are now known, the periodogram can be computed through the following Expression:

$$\mathbf{Per}(\theta) = \frac{1}{N_R} \left| \mathbf{a}_R(\theta)^H \mathbf{y}_R \right|^2 \frac{1}{N_{tx}} \tag{3.13}$$

Where N_R is the size of the vector $\mathbf{y}_R$ and θ varies from -90º to 90º. Analyzing the periodogram across the θ range, the angle that maximizes $\mathbf{Per}(\theta)$ can be identified. This peak corresponds to the most likely angle of arrival. One of the key advantages of this estimation method is that it's computationally efficient and easy to implement.

3.4 Results

Table 3.1 presents the main parameters considered for the simulation. The system's performance was evaluated considering different parameter values for the number of AP antennas (N_{tx}) and the number of APs (M).

In both cases, two targets are considered: one has a reflectivity gain of 0 dB, and the other has a reflectivity gain of 20 dB. The noise power was set to 0 dB. The metrics for evaluating the system's performance are the BER and the periodogram, determining signal quality for the communications and for the Radar part, respectively.

Table 3.1: Static simulation parameters for the first case

Simulation parameters	
Number of UE's (U)	1
Number of transmitting antennas per UE (N_{ue})	1
Number of sub-carriers (k)	64
Modulation order	4 (QAM)
Carrier frequency (f)	28 GHz
Number of clusters (N_{cl})	5
Number of rays per clusters (N_{ray})	3
Angle spread (AngleSpread)	8º
Path-loss exponent (n_p)	4.1 dB
Standard deviation of shadowing factor (d_{p_s})	7.6 dB

3.4.1 Case 1

In this case, the number of APs (M) remains static and equal to 1, and the variable parameter is the number of AP antennas (N_{tx}):

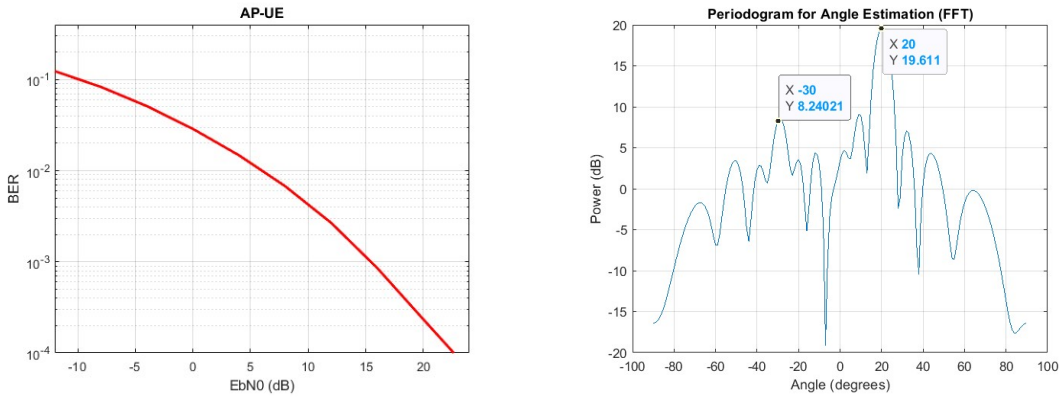

Figure 3.6: BER and periodogram for $N_{tx} = 16$

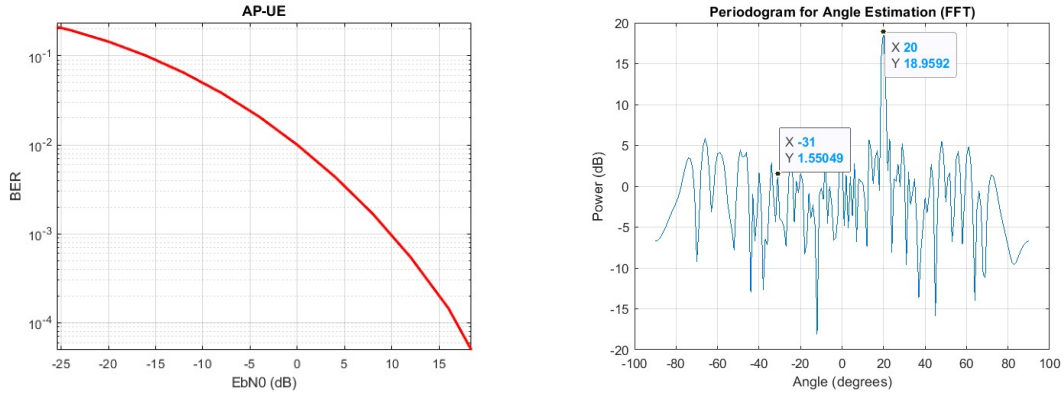

Figure 3.7: BER and periodogram for $N_{tx} = 64$

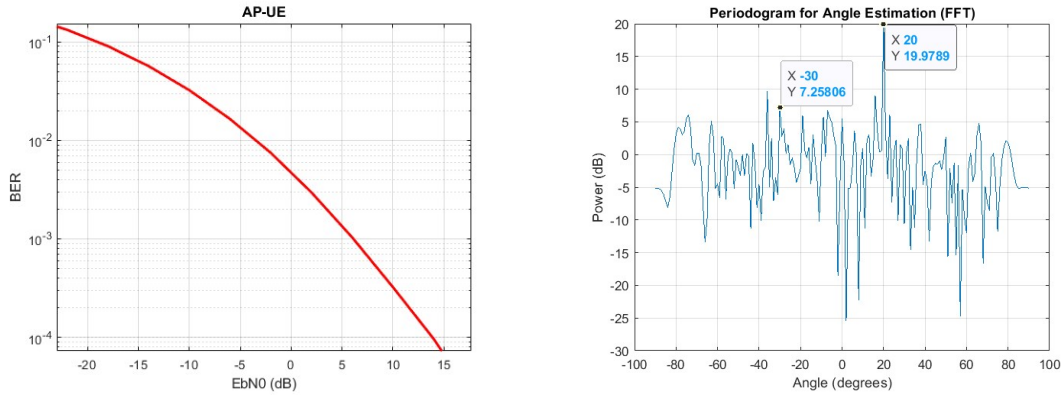

Figure 3.8: BER and periodogram for $N_{tx} = 128$

From the results shown in Figures 3.6, 3.7 and 3.8, when the number of antennas increases, the angle resolution is increased, which explains why the lobes in the periodogram of Figure 3.8 are much smaller than the ones in Figures 3.6 and 3.7.

This is expected, as it can be seen in the Expression (2.10) that the resolution increases with a greater number of antennas. The target at 20º is distinguishable from the noise, but the target at -30º is not, because its power is 0, just like the noise power - regardless of the number of antennas. This is also to be expected, as advantage cannot be taken from the diversity of multiple APs.

Regarding communications, as the number of antennas increases, the system's performance also increases, as it requires less energy per bit to achieve the 10^{-4} BER mark, due to antenna gains.

3.4.2 Case 2

In the second case, the number of APs (M) is variable, and the number of AP antennas (N_{tx}) remains static at 64.

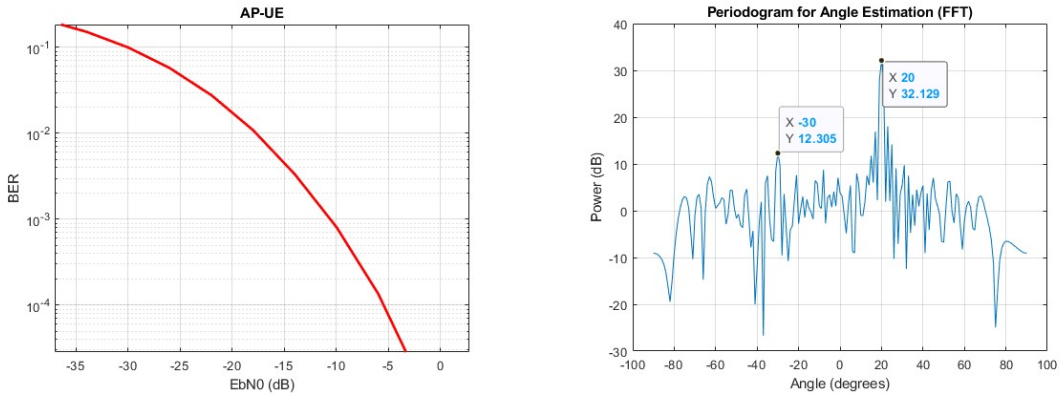

Figure 3.9: BER and periodogram for $M = 4$

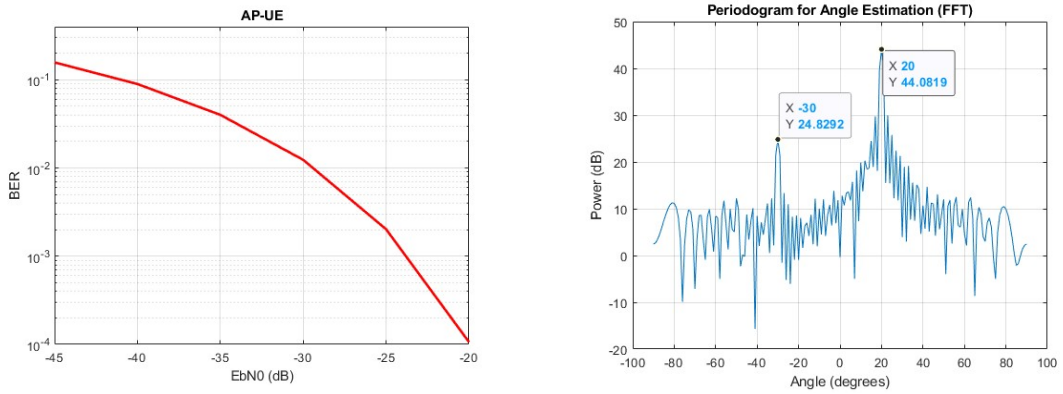

Figure 3.10: BER and periodogram for $M = 16$

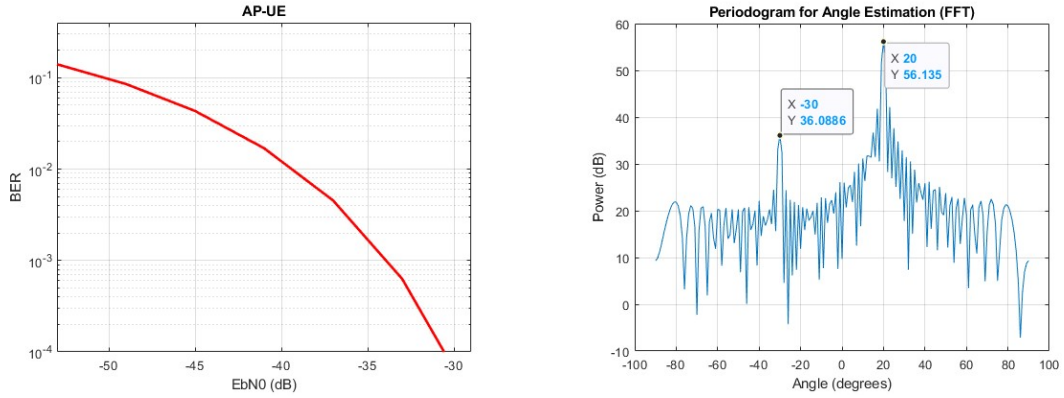

Figure 3.11: BER and periodogram for $M = 64$

In the second case, the Radar shows that (still with 0 dB reflective gain) the targets at 20º can be distinguished from noise. This is due to the diversity gains introduced by having more than a single transmitting AP. As these APs are cooperative, they are all connected to the same CU and share the same information, leading to power gains.

The power gain can be computed through the Expression below:

$$G = 20 \log_{10}(10^{\frac{r}{20}} M) \text{ dB} \tag{3.14}$$

Where M is the number of transmitting APs and r is the reflectivity gain, which differs for each target. From the results in Figure 3.9, it can be seen that in case 1, where the signal was obfuscated by noise, the target is now distinguishable due to AP cooperation, which leads to diversity gains. Using Equation 3.14, a 12 dB gain can be observed. The target with a reflectivity gain of 20 dB also undergoes a significant improvement, boosting its gain to 32 dB.

Now observing Figure 3.10, an improvement is seen, as the number of APs increases. The 20º target is now clearly distinguished from the noise and has a 25 dB gain increase, as does the 30º target. Finally, the best results are seen in Figure 3.11, which is to be expected since the simulation instances the most APs. The angle resolution is the same in all simulations, as seen by the width of the lobes on the periodogram - this is expected, as the number of antennas on each AP is static and the number of APs does not affect the angle resolution.

Communications results show that as the number of APs increases, the system's performance also increases, due to not only the spatial gain from using several APs but also the employed precoders, which exploit channel diversity and thus improve its robustness against fading.

Chapter 4

Final remarks and future work

The future of Integrated Sensing and Communications promises to revolutionize wireless networks by seamlessly integrating sensing capabilities into communications systems. This integration will enable next-generation networks, such as 6G, to support a wide array of applications, including autonomous vehicles, smart cities, and advanced IoT solutions. Combining this technology with a Cell-Free architecture is an exciting prospect for the future of mobile communications. This document focused on the downlink direction of an ISAC system with cooperative transmitting beamforming.

This final chapter comprises the conclusions obtained from this work and some relevant aspects for future work development.

4.1 Final remarks

This dissertation proposed a CF ISAC system with cooperative transmitting beamforming. ISAC systems are characterized by performing sensing and communications simultaneously, leveraging shared hardware to do this.

Cooperative beamforming involves transmitting signals from antennas in a way that creates constructive interference - this is enabled by the Cell-Free architecture, as every AP is connected to the same CU (shared knowledge). The joint waveform is divided into some sub-carriers with the communications component and others with the Radar component. Regarding the former, a fully digital precoder was considered, using the MMSE algorithm. The Radar precoder comprises the transmitting steering vector.

Concerning the results, two cases were presented: the first showed an increase in the number of antennas in each AP while keeping the number of APs constant; the second case involved a constant number of antennas in each AP and a progressive increase in the number of APs. Every other parameter between these two cases remained the same, meaning the system was evaluated regarding variations in the number of APs (M) and transmitting antennas (N_{tx}).

The results showed:

- An increase in the number of transmitting antennas reflected a higher angle resolution, as the periodogram's lobes were much narrower. The increase of transmitting antennas also brought benefits to the communications component, with improved energy efficiency and performance due to both diversity and antenna gains, allowing the system to achieve lower BER at reduced energy costs;
- Fostering AP cooperation, the system's performance can be enhanced by boosting received signal power and transforming previously indiscernible targets into distinguishable ones, despite the presence of noise;
- Increasing the number of APs leads to greater diversity gains, more effective interference management, and better power gains, which benefits both Radar and communications tasks.

In conclusion, this system demonstrates significant performance advantages by leveraging cooperative APs. As the number of APs increases, so does the robustness of the system, offering diversity and spatial gains that improve target detection and communications. The increased number of antennas enhances angle resolution, enabling a more effective distinction of targets. Finally, the system benefits from lower energy consumption on the communications front, highlighting its efficiency.

4.2 Future work

The main purpose of this dissertation was to implement a CF ISAC system with cooperative beamforming, with a great emphasis on angle detection. There are several aspects related to this topic that can lead to the development of further research. As such, below are two main examples that can be studied in future work in order to have a more complete Radar:

- Further developing this system so it can account for target distance, as well as relative velocity;
- Evaluating other algorithms for angle estimation, such as Multiple Signal Classification (MUSIC) and Estimation of Signal Parameters via Rotational Invariant Techniques (ESPRIT).

References

[1] M. Attaran, "The impact of 5G on the evolution of intelligent automation and industry digitization," *Journal of Ambient Intelligence and Humanized Computing*, vol. 14, 02 2021.

[2] T. Mshvidobadze, "Evolution mobile wireless communication and lte networks," in *2012 6th International Conference on Application of Information and Communication Technologies (AICT)*, 2012, pp. 1–7.

[3] D. Gowda, K. Sudhindra, B. Harshitha, H. Surendra., and K. Madhusudhan., "Evolution of mobile communication leading to 5G," in *2021 5th International Conference on Electrical, Electronics, Communication, Computer Technologies and Optimization Techniques (ICEECCOT)*, 2021, pp. 813–819.

[4] A. F. M. Shahen Shah, "A Survey From 1G to 5G Including the Advent of 6G: Architectures, Multiple Access Techniques, and Emerging Technologies," in *2022 IEEE 12th Annual Computing and Communication Workshop and Conference (CCWC)*, 2022, pp. 1117–1123.

[5] Q. K. Ud Din Arshad, A. U. Kashif, and I. M. Quershi, "A review on the evolution of cellular technologies," in *2019 16th International Bhurban Conference on Applied Sciences and Technology (IBCAST)*, 2019, pp. 989–993.

[6] DevX. (2023) Interim standard 95 (is-95). Accessed: 2024-09-06. [Online]. Available: https://www.devx.com/terms/interim-standard-95/

[7] 3rd Generation Partnership Project (3GPP). (2024) Introducing 3GPP. https://www.3gpp.org/about-us/introducing-3gpp. Accessed on: 2024-02-09.

[8] I. Ganchev, M. O'Droma, H. Chaouchi, I. Armuelles, M. Siebert, and N. Houssos, "Requirements for an integrated system and service 4G architecture," in *2004 IEEE 59th Vehicular Technology Conference. VTC 2004-Spring (IEEE Cat. No.04CH37514)*, vol. 5, 2004, pp. 3029–3034 Vol.5.

[9] S. Chen, S. Sun, Y. Wang, G. Xiao, and R. Tamrakar, "A comprehensive survey of TDD-based mobile communication systems from TD-SCDMA 3G to TD-LTE(A) 4G and 5G directions," *China Communications*, vol. 12, no. 2, pp. 40–60, 2015.

[10] ETSI. (n.d.) 5G. Accessed: 2024-09-06. [Online]. Available: https://www.etsi.org/technologies/5G

[11] H. Kim, "Performance analysis of k means clustering algorithms for mmtc systems," in *2020 International Conference on Information and Communication Technology Convergence (ICTC)*, 2020, pp. 30–35.

[12] Q. Qiu, S. Liu, S. Xu, and S. Yu, "Study on Security and Privacy in 5G-Enabled Applications," *Wireless Communications and Mobile Computing*, vol. 2020, pp. 1–15, 12 2020.

[13] O. Aziz and M. Rahman, "Miniaturized four port mimo antenna for urllc and virtual mimo applications," in *2023 Photonics & Electromagnetics Research Symposium (PIERS)*, 2023, pp. 1029–1033.

[14] G. Liu, Y. Huang, Z. Chen, L. Liu, Q. Wang, and N. Li, "5G Deployment: Standalone vs. Non-Standalone from the Operator Perspective," *IEEE Communications Magazine*, vol. 58, no. 11, pp. 83–89, 2020.

[15] M. Guarnieri, "The early history of radar [historical]," *IEEE Industrial Electronics Magazine*, vol. 4, no. 3, pp. 36–42, 2010.

[16] V. H. Alves Ribeiro, G. Reynoso-Meza, and L. dos Santos Coelho, "Chapter 10 - multiobjective optimization design procedures for data-driven unmanned aerial vehicles automatic target recognition systems," in *Unmanned Aerial Systems*, ser. Advances in Nonlinear Dynamics and Chaos (ANDC), A. Koubaa and A. T. Azar, Eds. Academic Press, 2021, pp. 231–256. [Online]. Available: https://www.sciencedirect.com/science/article/pii/B9780128202760000170

[17] Y. Blanchard, "Une histoire du radar en lien avec les mutations du système technique," *Revue de l'Electricité et de l'Electronique*, vol. 2019, pp. 35–46, July 2019.

[18] D. K. A. Pulutan and J. S. Marciano, "Design trade-offs in a combined fmcw and pulse doppler radar front-end," in *IEEE 2013 Tencon - Spring*, 2013, pp. 567–571.

[19] H. Griffiths, "Early history of bistatic radar," in *2016 European Radar Conference (EuRAD)*, 2016, pp. 253–257.

[20] H. Aziz, M. Hazwan, N. E. RASHID, r. s. a. raja abdullah, K. Othman, and A. Salah, "Rcs analysis on different targets and bistatic angles using lte frequency," vol. 3, 06 2015, pp. 658–663.

[21] H. Griffiths, "Bistatic radar - principles and practice," in *SBMO International Microwave Conference/Brazil,*, vol. 2, 1993, pp. 519–526.

[22] ——, "Klein heidelberg: New information and insight," in *2015 IEEE Radar Conference*, 2015, pp. 527–532.

[23] J. Kim and Y. K. Kwag, "Interference effect analysis from ground based radar in high resolution spaceborne sar image," in *2011 3rd International Asia-Pacific Conference on Synthetic Aperture Radar (APSAR)*, 2011, pp. 1–4.

[24] M. Z. Butt and S. T. Gul, "Range and doppler estimation of multiple moving targets for pulsed doppler radars with cfar detector at very low snrs," in *2014 International Conference on Emerging Technologies (ICET)*, 2014, pp. 147–152.

[25] L. Zhang, W. Zhao, A. Cao, and C. He, "Single-channel monopulse tracking receiver with time modulation," in *2022 IEEE International Symposium on Antennas and Propagation and USNC-URSI Radio Science Meeting (AP-S/URSI)*, 2022, pp. 1316–1317.

[26] Q. Jiang, R. Wang, W. Zhang, L. Jiao, W. Li, C. Wu, and C. Hu, "Monitoring dynamically changing migratory flocks using an algebraic graph theory-based clustering algorithm," *Remote Sensing*, vol. 16, p. 1215, 03 2024.

[27] R. Bil and W. Holpp, "Modern phased array radar systems in germany," in *2016 IEEE International Symposium on Phased Array Systems and Technology (PAST)*, 2016, pp. 1–7.

[28] W. Wiesbeck and L. Sit, "Radar 2020: The future of radar systems," in *2014 International Radar Conference*, 2014, pp. 1–6.

[29] R. M. Mealey, "A method for calculating error probabilities in a radar communication system," *IEEE Transactions on Space Electronics and Telemetry*, vol. 9, no. 2, pp. 37–42, 1963.

[30] F. Liu, Y. Cui, C. Masouros, J. Xu, T. X. Han, Y. C. Eldar, and S. Buzzi, "Integrated sensing and communications: Toward dual-functional wireless networks for 6g and beyond," *IEEE Journal on Selected Areas in Communications*, vol. 40, no. 6, pp. 1728–1767, 2022.

[31] H. Alyasiri, J. A. Clark, A. Malik, and R. d. Fréin, "Grammatical evolution for detecting cyberattacks in internet of things environments," in *2021 International Conference on Computer Communications and Networks (ICCCN)*, 2021, pp. 1–6.

[32] J. A. Zhang, M. L. Rahman, K. Wu, X. Huang, Y. J. Guo, S. Chen, and J. Yuan, "Enabling joint communication and radar sensing in mobile networks—a survey," *IEEE Communications Surveys & Tutorials*, vol. 24, no. 1, pp. 306–345, 2022.

[33] H. A. Ammar, R. Adve, S. Shahbazpanahi, G. Boudreau, and K. V. Srinivas, "User-centric cell-free massive mimo networks: A survey of opportunities, challenges and solutions," *IEEE Communications Surveys & Tutorials*, vol. 24, no. 1, pp. 611–652, 2022.

[34] O. T. Demir, E. Bjornson, and L. Sanguinetti, "Foundations of user-centric cell-free massive mimo," *Foundations and Trends in Signal Processing*, vol. 14, no. 3–4, p. 162–472, 2021. [Online]. Available: http://dx.doi.org/10.1561/2000000109

[35] S. B. Weinstein, "The history of orthogonal frequency-division multiplexing [history of communications]," *IEEE Communications Magazine*, vol. 47, no. 11, pp. 26–35, 2009.

[36] M. H. Mahmud, M. M. Hossain, A. A. Khan, S. Ahmed, M. A. Mahmud, and M. H. Islam, "Performance analysis of ofdm, w-ofdm and f-ofdm under rayleigh fading channel for 5g wireless communication," in *2020 3rd International Conference on Intelligent Sustainable Systems (ICISS)*, 2020, pp. 1172–1177.

[37] S. Kamal, C. Azurdia-Meza, and K. Lee, "Family of nyquist-i pulses to enhance orthogonal frequency division multiplexing system performance," *IETE Technical Review*, vol. 33, 02 2016.

[38] ——, "Family of nyquist-i pulses to enhance orthogonal frequency division multiplexing system performance," *IETE Technical Review*, vol. 33, 02 2016.

[39] D. A. ao Silva and D. A. Gameiro, "Comunicações sem fios (wireless communications)," *DETI, Universidade de Aveiro*, 2023.

[40] (n.d.) Concepts of orthogonal frequency division multiplexing (ofdm) and 802.11 wlan. Accessed: 2024-07-23. [Online]. Available: https://helpfiles.keysight.com/csg/89600B/Webhelp/Subsystems/wlan-ofdm/content/ofdm_basicprinciplesoverview.html

[41] S. Weinstein and P. Ebert, "Data transmission by frequency-division multiplexing using the discrete fourier transform," *IEEE Transactions on Communication Technology*, vol. 19, no. 5, pp. 628–634, 1971.

[42] L. Litwin and M. Pugel, "The principles of ofdm," *RF signal processing*, vol. 2, pp. 30–48, 2001.

[43] T. J. Rouphael, "Chapter 3 - common digital modulation methods," in *RF and Digital Signal Processing for Software-Defined Radio*, T. J. Rouphael, Ed. Burlington: Newnes, 2009, pp. 25–85. [Online]. Available: https://www.sciencedirect.com/science/article/pii/B9780750682107000035

[44] N. Belwal, G. S. Jethi, P. K. Juneja, and V. Joshi, "Investigating the impact of doppler shift performance of multipath rayleigh fading channel," in *2020 IEEE 5th International Conference on Computing Communication and Automation (ICCCA)*, 2020, pp. 473–476.

[45] M. Koohestani, A. Hussain, A. A. Moreira, and A. K. Skrivervik, "Diversity gain influenced by polarization and spatial diversity techniques in ultrawideband," *IEEE Access*, vol. 3, pp. 281–286, 2015.

[46] A. Y. Hassan, "A frequency-diversity system with diversity encoder and ofdm modulation," *IEEE Access*, vol. 9, pp. 2805–2818, 2021.

[47] F. Adachi and R. Takahashi, "User-driven suboptimal joint transmit-receive diversity in asymmetric mimo fading channel," in *2022 27th Asia Pacific Conference on Communications (APCC)*, 2022, pp. 214–219.

[48] J. Winters, "The diversity gain of transmit diversity in wireless systems with rayleigh fading," *IEEE Transactions on Vehicular Technology*, vol. 47, no. 1, pp. 119–123, 1998.

[49] F. Laakso, P. Eskelinen, and M. Lampinen, "Uplink weight signaling for hsupa closed loop transmit diversity," in *2012 IEEE 23rd International Symposium on Personal, Indoor and Mobile Radio Communications - (PIMRC)*, 2012, pp. 2248–2252.

[50] (n.d.) Mimo spatial multiplexing. Accessed: 2024-07-30. [Online]. Available: https://www.electronics-notes.com/articles/antennas-propagation/mimo/spatial-multiplexing.php

[51] L. Zheng and D. Tse, "Diversity and multiplexing: a fundamental tradeoff in multiple-antenna channels," *IEEE Transactions on Information Theory*, vol. 49, no. 5, pp. 1073–1096, 2003.

[52] K. Wang, D. Yang, S. Babakhanov, E. Chatziaristotle, S. Sen, and M. Brockschmidt, "Open vocabulary learning on source code with a graph-augmented abstract syntax tree model," 2021.

[53] H. Yu, L. Zhong, and A. Sabharwal, "Power management of mimo network interfaces on mobile systems," *IEEE Transactions on Very Large Scale Integration Systems - VLSI*, vol. 20, pp. 1175–1186, 07 2012.

[54] F. A. Pereira de Figueiredo, "An Overview of Massive MIMO for 5G and 6G," *IEEE Latin America Transactions*, vol. 20, no. 6, pp. 931–940, 2022.

[55] G. Femenias and F. Riera-Palou, "Wideband cell-free mmwave massive mimo-ofdm: Beam squint-aware channel covariance-based hybrid beamforming," *IEEE Transactions on Wireless Communications*, vol. 21, no. 7, pp. 4695–4710, 2022.

[56] V. Verma and D. Sharma, "Improvement in quality of service of manet routing through convergence of mobile software agent," Ph.D. dissertation, Rajasthan Technical University, 01 2020.

[57] J. Zong, Y. Liu, H. Liu, Q. Wang, and P. Chen, "6g cell-free network architecture," in *2022 IEEE 2nd International Conference on Electronic Technology, Communication and Information (ICETCI)*, 2022, pp. 421–425.

[58] H. Griffiths, "From a different perspective: principles, practice and potential of bistatic radar," in *2003 Proceedings of the International Conference on Radar (IEEE Cat. No.03EX695)*, 2003, pp. 1–7.

[59] G. An, Z. Huang, and Y. Li, "Constant false alarm rate detection of pipeline leakage based on acoustic sensors," *Scientific Reports*, vol. 13, 08 2023.

[60] (n.d.) Pulse radar. Accessed: 2024-08-26. [Online]. Available: https://www.britannica.com/technology/radar/Pulse-radar

[61] Christisan Wolff. (n.d.) Radar basics. Accessed: 2024-08-26. [Online]. Available: https://www.radartutorial.eu/01.basics/Range%20Resolution.en.html

[62] C. Fulton, P. Kenworthy, J. Lujan, M. Herndon, S. Garner, D. Thompson, and M. Yeary, "Mutual coupling-based calibration for the horus digital phased array radar," in *2022 IEEE International Symposium on Phased Array Systems & Technology (PAST)*, 2022, pp. 1–6.

[63] Carolyn Mathas. (n.d.) Phased array antennas. Accessed: 2024-08-26. [Online]. Available: https://www.planetanalog.com/phased-array-antennas-from-military-to-5g/

[64] Y. L. Sit, T. T. Nguyen, C. Sturm, and T. Zwick, "2d radar imaging with velocity estimation using a mimo ofdm-based radar for automotive applications," in *2013 European Radar Conference*, 2013, pp. 145–148.

[65] Sandeep Rao. (n.d.) Mimo radar. Accessed: 2024-08-27. [Online]. Available: https://www.ti.com/lit/pdf/swra554

[66] Q. Chaudhari. (2022) Fmcw radar part 3: Design guidelines. Accessed: 2024-10-22. [Online]. Available: https://wirelesspi.com/fmcw-radar-part-3-design-guidelines/

[67] K. Braun and F. Jondral, *OFDM Radar Algorithms in Mobile Communication Networks*, ser. Forschungsberichte aus dem Institut für Nachrichtentechnik des Karlsruher Instituts für Technologie. KIT-Bibliothek, 2014. [Online]. Available: https://books.google.pt/books?id=8FXVzQEACAAJ

[68] A. M. Haimovich, R. S. Blum, and L. J. Cimini, "Mimo radar with widely separated antennas," *IEEE Signal Processing Magazine*, vol. 25, no. 1, pp. 116–129, 2008.